JOC Article

Diastereoselective Synthesis of Piperidine Imino Sugars Using Aldol Additions of Metalated Bislactim Ethers to Threose and Erythrose Acetonides

María Ruiz,* Tania M. Ruanova, Olga Blanco, Fátima Núñez, Cristina Pato, and Vicente Ojea*

Departamento de Química Fundamental, Facultade de Ciencias, Universidade da Coruña, Campus da Zapateira s/n, 15071 A Coruña, Spain

ruizpr@udc.es; ojea@udc.es

Received December 5, 2007

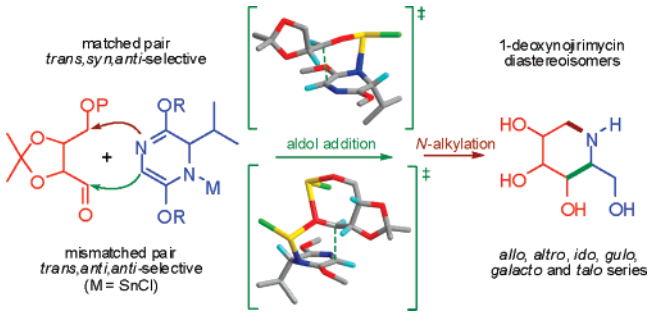

A general strategy for the synthesis of 1-deoxy-azasugars from a chiral glycine equivalent and 4-carbon building blocks is described. Diastereoselective aldol additions of metalated bislactim ethers to matched and mismatched erythrose or threose acetonides and intramolecular *N*-alkylation (by reductive amination or nucleophilic substitution) were used as key steps. The dependence of the yield and the asymmetric induction of the aldol addition with the nature of the metallic counterion of the azaenolate and the γ-alkoxy protecting group for the erythrose or threose acetonides has been studied. The stereochemical outcome of the aldol additions with tin(II) azaenolates has been rationalized with the aid of density functional theory (DFT) calculations. In accordance with DFT calculations with model glyceraldehyde acetonides, high *trans,syn,anti*-selectivitity for the matched pairs and moderate to low *trans,anti,anti*-selectivity for the mismatched ones may originate from (1) the intervention of solvated aggregates of tin(II) azaenolate and lithium chloride as the reactive species and (2) favored chair-like transition structures with a Cornforth-like conformation for the aldehyde moiety. DFT calculations indicate that aldol additions to erythrose acetonides proceed by an initial deprotonation, followed by coordination of the alkoxy-derivative to the tin(II) azaenolate and final reorganization of the intermediate complex through pericyclic transition structures in which the erythrose moiety is involved in a seven-membered chelate ring. The preparative utility of the aldol-based approach was demonstrated by application in concise routes for the synthesis of the glycosidase inhibitors 1-deoxy-D-allonojirimycin, 1-deoxy-L-altronojirimycin, 1-deoxy-D-gulonojirimycin, 1-deoxy-D-galactonojirimycin, 1-deoxy-L-idonojirimycin and 1-deoxy-D-talonojirimycin.

Introduction

Glycobiology is a rapidly growing research area uncovering multiple biological processes wherein carbohydrates play a major role. Natural and synthetic alkaloidal sugar mimics with a nitrogen in the ring (imino sugars, commonly named as aza sugars)[1] have emerged as important tools for glycobiology research.[2] The substitution of the ring oxygen of the sugars with the nitrogen renders the imino sugars metabolically inert but does not prevent their recognition by glycoprocessing enzymes. When protonated, imino sugars resemble the transient oxocar-

(1) Although in broad usage, the term aza sugar is incorrect. It should be restricted to structures where carbon, not oxygen, is replaced by a nitrogen. For IUPAC recommendations on the nomenclature of carbohydrates, see: *Pure Appl. Chem.* **1996**, *68*, 1919−2008.

(2) Dwek, R. A. *Chem. Rev.* **1996**, *96*, 683−720.

10.1021/jo702601z CCC: $40.75
Published on Web 02/27/2008

CHART 1

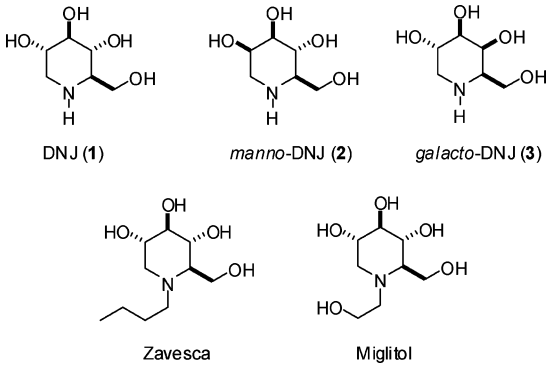

CHART 2

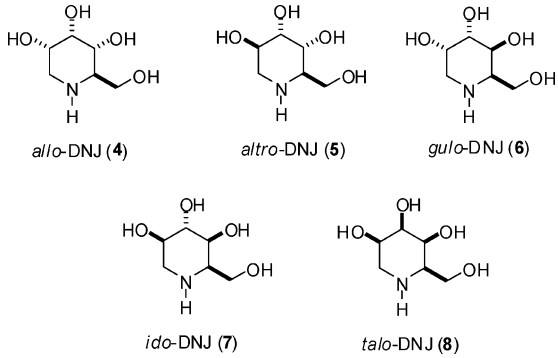

bonium ion involved in glycoside hydrolysis and thus can act as transition-state analogues for the competitive inhibition of the glycosidases and glycosyltransferases. Inhibition of these enzymes affects the maturation, transport, secretion, and function of glycoproteins and could alter cell−cell or cell−virus recognition processes. Therefore, glycosidase inhibitors have been shown to interact with receptors related to a wide range of prominent diseases including viral infections, cancer, diabetes and other metabolic disorders and are expected to find an increasing number of applications as beneficial drugs.[3]

Inhibitors of glycosidases that are essential for survival, such as the archetypal 1-deoxynojirimycin (DNJ, **1**), *manno*-DNJ (**2**), or *galacto*-DNJ (**3**), have been extensively studied in synthetic chemical[4−6] and biochemical laboratories (see Chart 1). Thus, *N*-butyl-DNJ (Zavesca) and *N*-hydroxyethyl-DNJ (Miglitol or Glyset)[7] have been already approved for the treatment of diabetes type 1, Gaucher disease, and lysosomal storage disorder, and *galacto*-DNJ (AT1001) is currently in phase B clinical trials for the treatment of Fabry's disease.[8] Conversely, other diastereoisomers of DNJ have received less synthetic attention, and therefore, there are few reports on glycosidase inhibition by *allo*-DNJ (**4**),[9] *altro*-DNJ (**5**),[10,11] *gulo*-DNJ (**6**),[12,13] *ido*-DNJ (**7**),[14,15] and *talo*-DNJ (**8**,[16,17] see Chart 2).[18]

Although traditionally polyhydroxylated piperidines have been synthesized through enantiospecific transformations of

(3) (a) Asano, N. *Glycobiology* **2003**, *13*, 93R−104R. (b) Martin, O. R., Compain, P., Eds.; Iminosugars: Recent Insights into their Bioactivity and Potential as Therapeutic Agents. *Curr. Top. Med. Chem.* **2003**, *3* (5). (c) Watson, A. A.; Fleet, G. W. J.; Asano, N.; Molyneux, R. J.; Nash, R. J. *Phytochemistry* **2001**, *56*, 265−295. (d) *Iminosugars as Glycosidase Inhibitors: Nojirimicyn and Beyond*; Stütz, A. E., Ed.; Wiley-VCH: Weinheim, 1999.

(4) For recent reviews on the synthesis of polyhydroxylated piperidines and other imino sugars, see: (a) Afarinkia, K.; Bahar, A. *Tetrahedron: Asymmetry* **2005**, *16*, 1239−1287. (b) Pearson, M. S. M.; Mathé-Allainmat, M.; Fargeas, V.; Lebreton, J. *Eur. J. Org. Chem.* **2005**, 2159−2191. (c) Cipolla, L.; La Ferla, B.; Nicotra, F. *Curr. Top. Med. Chem.* **2003**, *3*, 485−511.

(5) Enantiospecific (carbohydrate-based) synthesis of *galacto*-DNJ: (a) Paulsen, H.; Hayauchi, Y.; Sinnwell, V. *Chem. Ber.* **1980**, *113*, 2601−2608. (b) Legler, G.; Pohl, S. *Carbohydr. Res.* **1986**, *155*, 119−129. (c) Bernotas, R. C.; Pezzone, M. A.; Ganem, B. *Carbohydr. Res.* **1987**, *167*, 305−311. (d) Furneaux, R.; Tyler, P. C.; Whitehouse, L. A. *Tetrahedron Lett.* **1993**, *34*, 3609−3612. (e) Shilvock, J. P.; Fleet, G. W. J. *Synlett* **1998**, 554−557. (f) Uriel, C.; Santoyo-Gonzalez, F. *Synlett* **1999**, 593−595. (g) McDonnell, C.; Cronin, L.; O'Brien, J. L.; Murphy, P. V. *J. Org. Chem.* **2004**, *69*, 3565−3568.

(6) Diastereoselective routes to *galacto*-DNJ: (a) Aoyagi, S.; Fujimaki, S.; Yamazaki, N.; Kibayashi, C. *J. Org. Chem.* **1991**, *56*, 815−819. (b) Liu, K. K.-C.; Kajimoto,T.; Chen, L.; Zhong, Z.; Ichikawa, Y.; Wong, C.-H. *J. Org. Chem.* **1991**, *56*, 6280−6289. (c) Lees, W. J.; Whitesides, G. M. *Bioorg. Chem.* **1992**, *20*, 173−179. (d) Chida, N.; Tanikawa, T.; Tobe, T.; Ogawa, S. *J. Chem. Soc., Chem. Commun.* **1994**, 1247−1248. (e) Johnson, C. R.; Golebiowski, A.; Sundram, H.; Miller, M. W.; Dwaihy, R. *Tetrahedron Lett.* **1995**, *36*, 653−654. (f) Asano, K.; Hakogi, T.; Iwama, S.; Katsumura, S. *Chem. Commun.* **1999**, 41−42. (g) Mehta, G.; Mohal, N. *Tetrahedron Lett.* **2000**, *41*, 5741−5745. (h) Takahata, H.; Banba, Y.; Ouchi, H.; Nemoto, H. *Org. Lett.* **2003**, *5*, 2527−2529. (i) Pyun, S.-j.; Lee, K.-y.; Oh, C.-y.; Ham, W.-h. *Heterocycles* **2004**, *62*, 333−341.

(7) (a) Mitrakou, A.; Tountas, N.; Raptis, A. E.; Bauer, R. J.; Schulz, H.; Raptis, S. A. *Diabetic Med.* **1998**, *15*, 657−660. (b) Cox, T.; Lachmann, R.; Hollack, C.; Aerts, J.; van Weely, S.; Hrebicek, M.; Platt, F. M.; Butters, T. D.; Dwek, R.; Moyses, C.; Gow, L.; Elstein, D.; Zimran, A. *Lancet* **2000**, *355*, 1481−1485. (c) Butters, T. D.; Dwek, R. A.; Platt, F. M. *Curr. Top. Med. Chem.* **2003**, *3*, 561−574.

(8) (a) Fan, J.-Q.; Ishii, S.; Asano, N.; Suzuki, Y. *Nat. Med.* **1999**, *5*, 112−115. (b) See: http://www.clinicaltrials.gov/ct/gui/show/NCT00231036.

(9) Previous synthesis of *allo*-DNJ: (a) Altenbach, H.-J.; Himmeldirk, K. *Tetrahedron: Asymmetry* **1995**, *6*, 1077−1080. (b) Ikota, N.; Hirano, J.-i.; Gamage, R.; Nakagawa, H.; Hama-Inaba, H. *Heterocycles* **1997**, *46*, 637−643. (c) Wu, X.-D.; Khim, S.-K.; Zhang, X.; Cederstrom, E.; Mariano, P. S. *J. Org. Chem.* **1998**, *63*, 841−859. (d) Hong, B.-C.; Chen, Z.-Y.; Nagarajan, A.; Kottani, R.; Chavan, V.; Chen, W.-H.; Jiang, Y.-F.; Zhang, S.-C.; Liao, J.-H.; Sarshar, S. *Carbohydr. Res.* **2005**, *340*, 2457−2468. (e) Ghosh, S.; Shashidhar, J.; Dutta, S. K. *Tetrahedron Lett.* **2006**, *47*, 6041−6044. (f) Guaragna, A.; D'Errico, S.; D'Alonzo, D.; Pedatella, S.; Palumbo, G. *Org. Lett.* **2007**, *9*, 3473−3476.

(10) For a carbohydrate-based synthesis of *altro*-DNJ, see ref 5f.

(11) Diastereoselective synthesis of *altro*-DNJ: (a) Xu, Y.-M.; Zhou, W.-S. *J. Chem. Soc., Perkin Trans. 1* **1997**, 741−746. (b) Kazmaier, U.; Grandel, R. *Eur. J. Org. Chem.* **1998**, 1833−1840. (c) Takahata, H.; Banba, Y.; Sasatani, M.; Nemoto, H.; Kato, A.; Adachi, I. *Tetrahedron* **2004**, *60*, 8199−8205. (d) Dhavale, D. D.; Markad, S. D.; Karanjule, N. S.; PrakashaReddy, J. *J. Org. Chem.* **2004**, *69*, 4760−4766; see also refs 6b,f,g and 9f.

(12) Enantiospecific synthesis of *gulo*-DNJ: (a) Leontein, K.; Lindberg, B.; Lönngren, J. *Acta Chem. Scand. B* **1982**, *36*, 515−518. (b) Joseph, C. C.; Regeling, H.; Zwanenburg, B.; Chittenden, G. J. F. *Carbohydr. Res.* **2002**, *337*, 1083−1087. See also ref 9e.

(13) Diastereoselective synthesis of *gulo*-DNJ: (a) Liao, L.-X.; Wang, Z.-M.; Zhang, H.-X.; Zhou, W.-S. *Tetrahedron: Asymmetry* **1999**, *10*, 3649−3657. (b) Haukaas, M. H.; O'Doherty, G. A. *Org. Lett.* **2001**, *3*, 401−404. (c) Amat, M.; Huguet, M.; Llor, N.; Bassas, O.; Gómez, A. M.; Bosch, J.; Badia, J.; Baldoma, L.; Aguilar, J. *Tetrahedron Lett.* **2004**, *45*, 5355−5356. (d) Pyun, S.-J.; Lee, K.-Y.; Oh, C.-Y.; Joo, J.-E.; Cheon, S.-H.; Ham, W.-H. *Tetrahedron* **2005**, *61*, 1413−1416; see also ref 6h.

(14) Enantiospecific synthesis of *ido*-DNJ: (a) Fowler, P. A.; Haines, A. H.; Taylor, R. J. K.; Chrystal, E. J. T.; Gravestock, M. B. *Carbohydr. Res.* **1993**, *246*, 377−381. (b) Le Merrer, Y.; Poitout, L.; Depezay, J.-C.; Dosbaa, I.; Geoffroy, S.; Foglietti, M.-J. *Bioorg. Med. Chem.* **1997**, *5*, 519−533. (c) Hugel, H. M.; Hughes, A. B.; Khalil, K. *Aust. J. Chem.* **1998**, *51*, 1149−1155. (d) Lee, B. W.; Jeong, I.-Y.; Yang, M. S.; Choi, S. U.; Park, K. H. *Synthesis* **2000**, 1305−1309.

(15) Diastereoselective synthesis of *ido*-DNJ: (a) Dhavale, D. D.; Kumar, K. S. A.; Chaudhain, V. D.; Sharma, T.; Sabharwal, S. G.; PrakashaReddy, J. *Org. Biomol. Chem.* **2005**, *3*, 3720−3726. (b) Schaller, C.; Vogel, P.; Jäger, V. *Carbohydr. Res.* **1998**, *314*, 25−35. See also ref 6b,h.

(16) Carbohydrate-based synthesis of *talo*-DNJ: Hashimoto, H.; Hayakawa, M. *Chem. Lett.* **1989**, 1881−1884. See also ref 12b.

(17) Diastereoselective synthesis of *talo*-DNJ: C. R. Johnson, Golebiowski, A.; Schoffers, E.; Sundram, H.; Braun, M. P. *Synlett* **1995**, 313−314. See also refs 6b,c and 13a.

(18) Kato, A.; Kato, N.; Kano, E.; Adachi, I.; Ikeda, K.; Yu, L.; Okamoto, T.; Banba, Y.; Ouchi, H.; Takahata, H.; Asano, N. *J. Med. Chem.* **2005**, *48*, 2036−2044 and references therein.

SCHEME 1

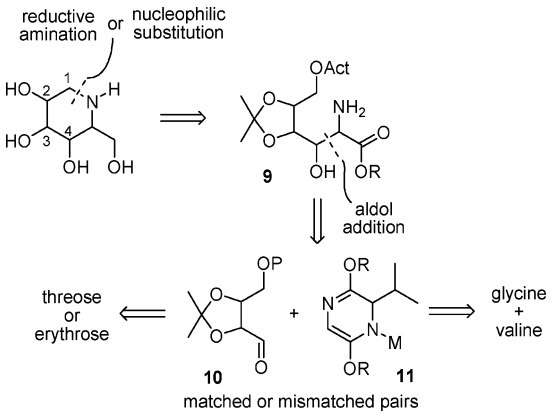

readily available carbohydrate precursors,[5,12,14,16] recent interest has increasingly focused on the stereoselective synthesis of this class of compounds.[19] Prominent among these strategies are cycloaddition-based routes,[20] chemoenzymatic functionalization of carbocyclic intermediates,[21,17] aldolase-catalyzed condensation reactions,[6b,c] and stereoselective elongation of homochiral short precursors exploiting different chemical procedures.[22] Moreover, in recent years, many efforts have been devoted to develop generally applicable and flexible methodologies, amenable to implementation of stereochemical variations for the asymmetric synthesis of any diastereoisomer of DNJ. Particularly useful among the general approaches are those relying on piperidene[23] or dihydropyridinone key intermediates, which can be prepared by stereoselective transformation of D-serine derivatives[24] or aza-Achmatowicz rearrangement of β-alkoxyfurfurylamines.[11a,13a,b]

As part of a project directed toward an efficient synthesis of bioactive amino polyol derivatives, we have recently developed a convergent approach to 2-amino-2-deoxyhexoses, where the stereoselective construction of the sugar backbone relied on an aldol reaction using derivatives of natural amino acids as chiral auxiliaries and building blocks.[25] Looking for a general and flexible methodology for the preparation of 1-deoxyazasugars of various configurations, we decided to extend the applicability of our aldol-based approach to amino sugars. In formulating the synthetic plan, we recognized that polyhydroxy amino acids **9** might be valuable key intermediates, since the targeted aza sugars would originate by cyclization, via reductive amination or nucleophilic substitution of an activated hydroxyl group, followed by reduction of the carboxylic acid group (see Scheme 1). We envisaged preparing key intermediates **9** from four-carbon building blocks and a chiral glycine equivalent by stereocontrolled aldol additions. Threose and erythrose derivatives **10** were sought as appropriate precursors, delivering various configurations at positions 2 and 3 and being suitably functionalized at positions 1 and 4. Moreover, additions to 2,3-*O*-isopropylidene-threose and -erythrose derivatives (such as **10**) proceed with variable stereoselectivity, which can be modulated by selecting the organometallic reagent.[26] On the other hand, we found Schöllkopf's bislactim ethers to be very attractive, a result of the high π-facial discrimination shown by these reagents in aldol-type reactions.[27] In particular, the reactions of titanium(IV), tin(II) or zinc(II) salts of bislactim ethers (such as **11**) with either matched or mismatched polyhydroxylated aldehydes have been reported to proceed under almost complete azaenolate control.[28,29] Surprisingly, until now there was only one other approach that relied on glycine as starting material for the synthesis of DNJ derivatives.[30] Kazmaier has reported an elegant synthesis of 1-deoxy-altronojirimycin[11b] using derivatives of L-tartaric acid as homologating reagents for *N*-tosylglycinate esters.

Thus, in this paper we wish to report in full details our results on the aldol reactions between metalated bislactim ethers derived from *cyclo*-[Gly-Val] and 2,3-*O*-isopropylidene-erythrose and -threose derivatives of complementary or non-complementary configurations.[31] To gain more insight into the origins of the stereoselection, we have also carried out a computational study of the possible reaction pathways, and transition-state models consistent with the stereochemical outcome of the aldol additions are also put forward. Finally, we demonstrate the general applicability of our aldol-based approach to piperidine imino sugars with an efficient transformation of the addition products into the six less-studied diastereoisomers of DNJ: D-*galacto*-

(19) Hudlicky, T.; Entwistle, D. A.; Pitzer, K. K.; Thorpe, A. J. *Chem. Rev.* **1996**, *96*, 1195−1220.

(20) See, for example: (a) Auberson, Y.; Vogel, P. *Angew. Chem., Int. Ed. Engl.* **1989**, *28*, 1498−1499. (b) Streith, J.; Defoin, A. *Synlett* **1996**, 189−200.

(21) See, for example: Hudlicky, T.; Rouden, J.; Luna, H.; Allen, S. *J. Am. Chem. Soc.* **1994**, *116*, 5099−5107.

(22) Casiraghi, G.; Zanardi, F.; Rassu, G.; Spanu, P. *Chem. Rev.* **1995**, *95*, 1677−1716.

(23) (a) Martín, R.; Moyano, A.; Pericàs, M. A.; Riera, A. *Org. Lett.* **2000**, *2*, 93−95. (b) Martín, R.; Murruzzu, C.; Pericàs, M. A.; Riera, A. *J. Org. Chem.* **2005**, *70*, 2325−2328. See also ref 9f.

(24) Subramanian, T.; Lin, C.-C.; Lin, C.-C. *Tetrahedron Lett.* **2001**, *41*, 4079−4082. See also refs 6f,h, 9a,c,f, and 18.

(25) (a) Ruiz, M.; Ojea, V.; Quintela, J. M. *Tetrahedron Lett.* **1996**, *37*, 5743−5746. (b) Ojea, V.; Ruiz, M.; Quintela, J. M. *Synlett* **1997**, 83−84. (c) Ruiz, M.; Ojea, V.; Quintela, J. M. *Tetrahedron: Asymmetry* **2002**, *13*, 1535−1549. (d) Ruiz, M.; Ojea, V.; Quintela, J. M. *Tetrahedron: Asymmetry* **2002**, *13*, 1863−1873.

(26) (a) Guillarme, S.; Plé, K.; Banchet, A.; Liard, A.; Haudrechy, A. *Chem. Rev.* **2006**, *106*, 2355−2403. (b) Evans, D. A.; Glorius, F;, Burch, J. D. *Org. Lett.* **2005**, *7*, 3331−3333. (c) Majewski, M.; Shao, J.; Nelson, K.; Nowak, P.; Irvine, N. M. *Tetrahedron Lett.* **1998**, *39*, 6787−6790. (d) Lehmann, T. E.; Berkessel, A. *J. Org. Chem.* **1997**, *62*, 302−309. (e) Pearson, W. H.; Hembre, E. J. *J. Org. Chem.* **1996**, *61*, 7217−7221. (f) Martin, S. F.; Chen, H.-J.; Lynch, V. M. *J. Org. Chem.* **1995**, *60*, 276−278. (g) Gallagher, T.; Giles, M.; Subramanian, R. S.; Hadley, M. S. *J. Chem. Soc., Chem. Commun.* **1992**, 166−168. (h) Mekki, B.; Singh, G.; Wightman, R. H. *Tetrahedron Lett.* **1991**, *32*, 5143−5146. (i) Mukaiyama, T.; Suzuki, K.; Yamada, T.; Tabusa, F. *Tetrahedron* **1990**, *46*, 265−276. (j) Bukownik, R. R.; Wilcox, C. S. *J. Org. Chem.* **1988**, *53*, 463−471. (k) Buchanan J. G.; Jigajinni, V. B.; Singh, G.; Wightman, R. H. *J. Chem. Soc., Perkin Trans. 1* **1987**, 2377−2383 and references therein. (l) Corey, E. J.; Pan, B.-C.; Duy, H. H.; Deardoff, D. R. *J. Am. Chem. Soc.* **1982**, *104*, 6816−6818.

(27) Williams, R. M. *Synthesis of Optically Active* α*-Amino Acids*; Baldwin, J. E., Magnus, P. D., Eds.; Organic Chemistry Series, Vol. 7; Pergamon: Oxford, 1989.

(28) (a) Grauert, M.; Schöllkopf, U. *Liebigs Ann. Chem.* **1985**, 1817−1824. (b) Depezay, J. C.; Dureault, A.; Prange, T. *Tetrahedron Lett.* **1984**, *25*, 1459−1462.

(29) (a) Kobayashi, S.; Furuta, T.; Hayashi, T.; Nishijima, M.; Hanada, K. *J. Am. Chem. Soc.* **1998**, *120*, 908−919. (b) Kobayashi, S.; Furuta, T. *Tetrahedron* **1998**, *54*, 10275−10294. (c) Kobayashi, S.; Matsumura, M.; Furuta, T.; Hayashi, T.; Iwamoto, S. *Synlett* **1997**, 301−303. See also: Cremonesi, G.; Dalla Croce, P.; Fontana, F.; Forni, A.; La Rosa, C. *Tetrahedron: Asymmetry* **2007**, *18*, 1667−1675.

(30) For conceptually related approaches to amino- or imino sugars, see: (a) Fujii, M.; Miura, T.; Kajimoto, T.; Ida, Y. *Synlett* **2000**, 1046−1048. (b) Polt, R.; Sames, D.; Chruma, J. *J. Org. Chem.* **1999**, *64*, 6147−6158. (c) Banfi, L.; Cardani, S.; Potenza, D.; Scolastico, C. *Tetrahedron* **1987**, *43*, 2317−2322. (d) Mukaiyama, T.; Miwa, T.; Nakatsuta, T. *Chem. Lett.* **1982**, 145−148.

(31) Part of this work was already presented as preliminary communications: (a) Ruiz, M.; Ojea, V.; Ruanova, T. M.; Quintela, J. M. *Tetrahedron: Asymmetry* **2002**, *13*, 795−799. (b) Ruiz, M.; Ojea, V.; Quintela, J. M. *Synlett* **1999**, 204−206. (c) Ruiz, M.; Ruanova, T.; Ojea, V.; Quintela, J. M. *Tetrahedron Lett.* **1999**, *40*, 2021−2024.

SCHEME 2 [a]

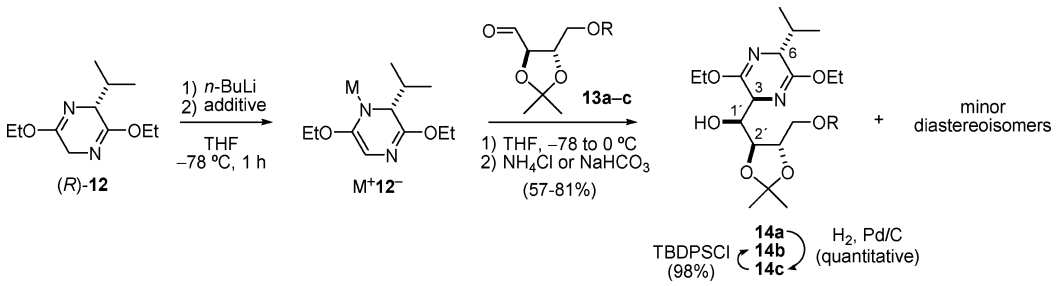

[a] Legend: **a**, R = Bn; **b**, R = $SiPh_2{}^tBu$; **c**, R = H.

SCHEME 3 [a]

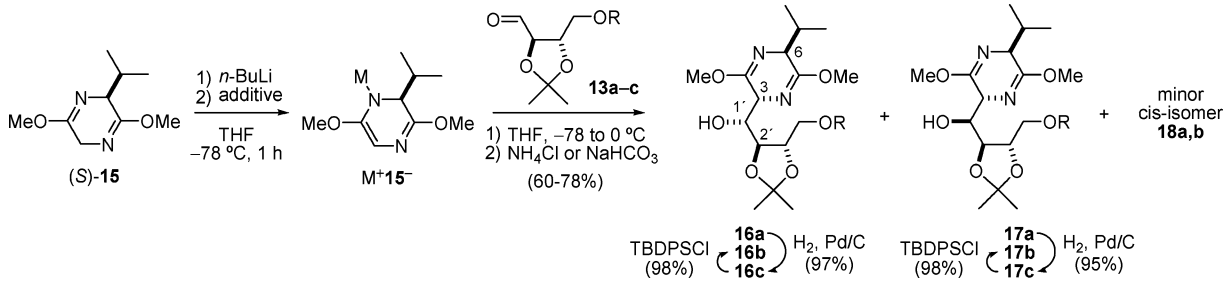

[a] Legend: **a**, R = Bn; **b**, R = $SiPh_2{}^tBu$; **c**, R = H.

DNJ (**3**), D-*allo*-DNJ (**4**), L-*altro*-DNJ (*ent*-**5**), D-*gulo*-DNJ (**6**), L-*ido*-DNJ (*ent*-**7**), and D-*talo*-DNJ (**8**).

Results and Discussion

1. Aldol Additions of Metalated Bislactim Ethers. 1.1. Aldol Additions to Threose Acetonides. We first examined the aldol additions of Schöllkopf's bislactim ethers derived from *cyclo*-[Gly-D-Val] and *cyclo*-[Gly-L-Val] ((*R*)-**12** and (*S*)-**15**), respectively) to L-threose acetonides **13a**−**c** (see Schemes 2 and 3). Benzyl and *tert*-butyldiphenylsilyl groups were selected to protect the γ-oxygen atom of the L-threose acetonides because of their synthetic utility and their significant steric and electronic differences. Thus, 4-*O*-benzyl- and 4-*O*-*tert*-butyldiphenylsilyl-2,3-*O*-isopropylidene-L-threose, **13a** and **13b**, respectively, were readily obtained from L-tartaric acid, following the reported procedures.[32a−c] Catalytic hydrogenation of **13a** gave 2,3-*O*-isopropylidene-L-threose[32d] (**13c**) in quantitative yield.

2,3-*O*-Isopropylidene derivatives of L-threose **13a**−**c** underwent stereoselective aldol additions of metalated azaenolates M^+**12**$^-$ and M^+**15**$^-$, in a fashion similar to that previously reported for other homochiral α,β-bisalkoxyaldehydes derived from glyceraldehyde[28] or threonine[25] or that were selected as convenient precursors for sphingofungins.[29] In this manner, slow addition of *n*-BuLi to a solution of bislactim ether (*R*)-**12** in THF at −78 °C was followed 1 h later by the dropwise addition of freshly distilled aldehydes **13a** or **13b**. Reactions took place at −78 °C within 2 h, and after quenching with NH_4Cl, aqueous workup, and removal of the excess of (*R*)-**12** by chromatography,[33] crude mixtures containing 3,6-*trans*-3,1′-*syn*-1′,2′-*anti* adducts **14a** or **14b** along with two other minor diastereoisomers were isolated in 64% or 57% combined yield (see Scheme 2 and Table 1). Integration of the pairs of doublets corresponding to the isopropyl groups in the ^{1}H NMR spectra of the mixtures of addition products revealed a moderate asymmetric induction in the formation of the new chiral centers. Thus, the diastereomeric ratios determined for the mixture of adducts obtained in the reactions of Li^+**12**$^-$ with the benzylated aldehyde **13a** and the silylated aldehyde **13b** were 77:15:8 and 60:20:20, respectively.

TABLE 1. Aldol Additions of M^+12**$^-$ to L-Threose Acetonides 13a−c**

(*R*)-**12** equiv	additive (equiv)	L-threose acetonide	(R)	yield[a]	ratio[b,c]
1.2		**13a**	(Bn)	64	77:15:8[d]
1.2	$SnCl_2$ (1.2)	**13a**	(Bn)	81	>98:2[d]
1.2		**13b**	(TBDPS)	57	60:20:20[d]
1.2	$SnCl_2$ (1.2)	**13b**	(TBDPS)	79	95:5[d]
3.0	$SnCl_2$ (3.0)	**13c**	(H)	76	87:10:3[e]

[a] Isolated yield of mixtures of diastereomeric adducts, after column chromatography. [b] Determined by integration of the ^{1}H NMR spectra of the crude mixtures. [c] Relative configurations of the minor diastereoisomers have not been assigned. [d] Reaction conducted at −78 °C in THF. [e] Reaction conducted from −78 to 0 °C in THF.

The separation of the major components of these mixtures could be achieved by flash chromatography, to provide adducts **14a** and **14b** of high purity, with a diastereomeric excess (de) higher than 98%. However, the selective formation of the major adducts could be increased by using a tin(II) azaenolate, as was previously reported by Kobayashi for related aldol additions.[29] Thus, lithium azaenolate Li^+**12**$^-$ was allowed to react with $SnCl_2$ for 1 h, in THF at −78 °C, to produce the transmetalated azaenolate $SnCl^+$**12**$^-$, prior to the addition of the aldehydes. Reactions of the tin(II) azaenolate with the benzylated and silylated acetonides **13a** and **13b** were complete under the

(32) (a) Martin, S. F.; Chen, H.-J.; Yang, C.-P. *J. Org. Chem.* **1993**, *58*, 2867−2873. (b) Uchida, K.; Kato, K.; Akita, H. *Synthesis* **1999**, 1678−1686. (c) Mash, E. A.; Nelson, K. A.; Van Deusen, S.; Hemperly, S. B. *Org. Synth.* **1990**, *68*, 92−103. (d) Morgenlie, S. *Carbohydr. Res.* **1985**, *138*, 329−334. (−)-Dimethyl 2,3-*O*-isopropylidene L-tartrate is commercially available from Fluka.

(33) The excess of Schöllkopf's reagent could be almost completely recovered and showed no racemization.

TABLE 2. Aldol Additions of M^+15^- to L-Threose Acetonides 13a−c

(*S*)-**15** equiv	additive (equiv)	L-threose acetonide	(R)	yield[a]	ratio **16/17/18**[b]
1.2		**13a**	(Bn)	60	49:37:14[c]
1.2	$SnCl_2$ (1.2)	**13a**	(Bn)	65	57:43:—[c]
1.2	$Sn(OTf)_2$ (1.2)	**13a**	(Bn)		
1.2	$ZnCl_2$ (1.2)	**13a**	(Bn)	46	40:42:18
1.2		**13b**	(TBDPS)	65	46:38:16[c]
1.2	$SnCl_2$ (1.2)	**13b**	(TBDPS)	78	57:35:8[c]
1.2	$SnCl_2$ (2.4)	**13b**	(TBDPS)	70	61:34:5[c]
1.2	Et_2AlCl (1.2)	**13b**	(TBDPS)	61	53:29:18[c]
1.2	$Ti(O^iPr)_3Cl$ (1.2)	**13b**	(TBDPS)	75	49:41:10[c]
3.0	$SnCl_2$ (3.0)	**13c**	(H)	62	50:50:—[d]

[a] Isolated yield of mixtures of diastereomeric adducts, after column chromatography. [b] Determined by integration of the ^1H NMR spectra of the crude mixtures. [c] Reaction conducted at −78 °C in THF. [d] Reaction conducted from −78 to 0 °C in THF.

standard conditions (−78 °C, THF, 2 h) and led, after quenching with $NaHCO_3$, aqueous workup, and removal of the excess of (*R*)-**12**,[33] to the corresponding adducts with higher yields and selectivities than with the lithium azaenolate. In this manner, by using $SnCl^+\mathbf{12}^-$, the aldol addition furnished the benzylated adduct **14a** as a single diastereoisomer (>98% de) in 81% isolated yield, while the silylated adduct **14b** was obtained in 79% yield with a de of 90%.

The influence of the protecting group for the primary hydroxyl group of the L-threose acetonides on the yield and the stereoselection of the aldol addition was further examined. As reactions of organometallic reagents with lactols are often more selective than reactions with the corresponding aldehydes,[34] the addition of the tin(II) azaenolate to 2,3-*O*-isopropylidene-L-threose (**13c**) was also studied. To this end, lactol **13c** was slowly added to a THF solution of 3 equiv of azaenolate $SnCl^+\mathbf{12}^-$ at −78 °C. As reaction was not observed after 2 h at −78 °C, the reaction mixture was gradually warmed to 0 °C. The addition of the tin(II) azaenolate to the lactol took place smoothly at temperatures higher than −30 °C, and total conversion was achieved after 5 h at 0 °C. In this conditions, after quenching of the reaction mixture with $NaHCO_3$, workup, and removal of the excess of (*R*)-**12** by chromatography,[33] a 87:10:3 mixture containing adduct **14c** along with two minor isomers could be isolated in 76% yield. Adducts **14b** and **14c** could also be prepared by monosilylation of **14c** and hydrogenation of **14a**, respectively (see Scheme 2 and part 3 of Results and Discussion).

Having shown the feasibility of performing stereoselective additions of azaenolates derived from bislactim ether (*R*)-**12** to L-threose derived acetonides, we explored the extension of this reactivity to the enantiomeric series of azaenolates, derived from bislactim ether (*S*)-**15**. The most salient results obtained in the aldol additions of mismatched azaenolates to the L-threose acetonides are given in Scheme 3 and Table 2. Upon addition of the protected aldehydes **13a** or **13b** to 1.2 equiv of $Li^+\mathbf{15}^-$ or $SnCl^+\mathbf{15}^-$ at −78 °C in THF, reactions also took place within 2 h. Conversely, reaction was not observed between $SnCl^+\mathbf{15}^-$ and lactol **13c** at low temperature, and thus the reaction mixture had to be gradually warmed to 0 °C during 12 h to produce the desired adducts. Surprisingly, reaction was not observed even in these conditions when the lithium azaenolate was allowed to react with tin(II) triflate in THF at −78 °C for 1 h prior to the addition of the aldehyde **13a**. After quenching, aqueous workup, and removal of the excess of bislactim ether (*S*)-**15**,[33] mixtures of the diastereomeric addition products **16**−**18** could be isolated in 60−78% combined yield. According to the ^1H NMR of the crude mixtures, additions of the mismatched lithium azaenolate $Li^+\mathbf{15}^-$ to either the benzylated or the silylated aldehydes (**13a** and **13b**) took place with low asymmetric induction in both new chiral centers and led to mixtures of the two possible 3,6-*trans* adducts (**16** and **17**, almost in a 1:1 ratio) along with small amounts of a 3,6-*cis* isomer (**18**). The use of the tin(II) azaenolate $SnCl^+\mathbf{15}^-$ resulted in higher yields and increased *trans*/*cis*-selectivity in the aldol addition to L-threose acetonides **13a**−**c**, although the ratio between the major adducts, 3,1′-*syn*-1′,2′-*syn*-**16a**−**c** and 3,1′-*anti*-1′,2′-*anti*-**17a**−**c**, were lower than 2:1 in all the cases. Prompted by the low stereoselectivity achieved in the azaenolate additions to the mismatched threose acetonides, we tested the process in the presence of other metallic counterions. Thus, we prepared the zinc(II), aluminum(III),[35] and the titanium(IV) azaenolates from $Li^+\mathbf{15}^-$ and $ZnCl_2$, Et_2AlCl, or $Ti(O^iPr)_3Cl$ (at −78 °C in THF), but their additions to the acetonides **13a** or **13b** also proceeded with low stereoselectivity and led to mixtures of the three adducts **16/17/18** with 40:42:18, 53:29:18 and 49:41:10 ratios, respectively. All mixtures of benzylated, silylated, or "unprotected" aldol products were separated by flash chromatography, and thus adducts **16a**−**c** and **17a**−**c** could be isolated as single diastereoisomers in 31−44% and 28−31% yield, respectively. Adducts **16b** and **17b** could also be prepared by monosilylation of **16c** and **17c**, respectively, and adducts **16c** and **17c** could also be prepared by hydrogenation of **16a** and **17a**, respectively (see Scheme 3 and part 3 of Results and Discussion).

SCHEME 4[a]

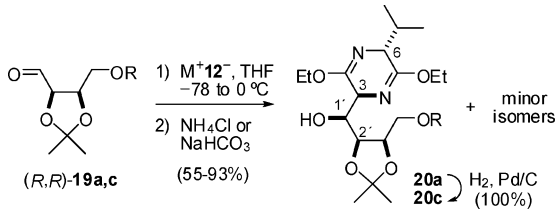

[a] Legend: **a**, R = Bn; **c**, R = H.

1.2. Aldol Additions to Erythrose Acetonides. To explore further the scope of these aldol reactions for the preparation of polyhydroxy amino acids, we examined the additions of metalated azaenolates $M^+\mathbf{12}^-$ to erythrose acetonides of the D- and L-series, with complementary or non-complementary configuration at the α-position, respectively. According to the literature, 2,3-*O*-isopropylidene-D-erythrose[36a] ((*R*,*R*)-**19c**, see Scheme 4) and its 4-*O*-benzyl derivative (*R*,*R*)-**19a**[36b] were prepared from D-isoascorbic acid and D-mannose, respectively, whereas 2,3-*O*-isopropylidene-L-erythrose[37] ((*S*,*S*)-**19c**, see Scheme 5) and its 4-*O*-benzyl derivative (*S*,*S*)-**19a**[38] were obtained from L-arabinose and L-rhamnose, respectively.

(34) See, for example: Berque, I.; Le Ménez, P.; Razon, P.; Mahuteau, J.; Férézou, J.-P.; Pancrazi, A.; Ardisson, J.; Brion, J.-D. *J. Org. Chem.* **1999**, *64*, 373−381. See also ref 26d,e,h.

(35) Andrews, P. C.; Maguire, M.; Pombo-Villar, E. *Eur. J. Inorg. Chem.* **2003**, *18*, 3305−3308.

(36) (a) Cohen, N.; Banner, B. L.; Laurenzano, A. J.; Carozza, L. *Organic Syntheses*; Wiley: New York, 1990; Collect. Vol. VII, pp 297−301. (b) Shen, X.; Wu, Y.-L.; Wu, Y. *Helv. Chim. Acta* **2000**, *83*, 943−953.

(37) Thompson, D. K.; Hubert, C. N.; Wightman, R. H. *Tetrahedron* **1993**, *49*, 3827−3840.

(38) Munier, P.; Krusinski, A.; Picq, D.; Anker, D. *Tetrahedron* **1995**, *51*, 1229−1244.

SCHEME 5 [a]

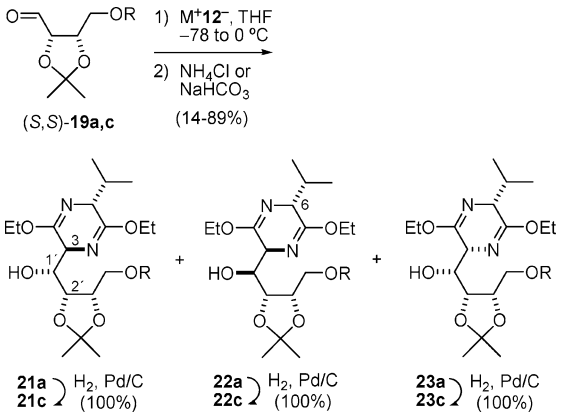

[a] Legend: **a**, R = Bn; **c**, R = H.

TABLE 3. Aldol Additions of M^+12^- to D-Erythrose Acetonides (*R*,*R*)-19a,c

(*R*)-**12** equiv	additive (equiv)	D-erythrose acetonide	(R)	yield[a]	ratio of adducts[b]
1.2		(*R*,*R*)-**19a**	(Bn)	69	89:11:—[c]
1.2	$SnCl_2$ (1.2)	(*R*,*R*)-**19a**	(Bn)	81	91:9:— [c]
3.0		(*R*,*R*)-**19c**	(H)	55	50:33:17[d]
3.0	$SnCl_2$ (3.0)	(*R*,*R*)-**19c**	(H)	93	>98:2:—[d]

[a] Isolated yield of mixtures of diastereomeric adducts, after column chromatography. [b] Determined by integration of the ^{1}H NMR spectra of the crude mixtures. [c] Reaction conducted at −78 °C in THF. [d] Reaction conducted from −78 to 0 °C in THF.

Reactions of 4-*O*-benzyl-2,3-*O*-isopropylidene-D-erythrose ((*R*,*R*)-**19a**) with 1.2 equiv of the lithium or the tin(II) azaenolates M^+**12**$^-$ in THF at −78 °C also took place within 2 h. The lithium azaenolate led, after quenching, aqueous workup, and removal of the excess of (*R*)-**12** by flash chromatography,[33] to a crude mixture containing the 3,6-*trans*-3,1′-*syn*-1,′2′-*anti* adduct **20a** along with a minor isomer, in a 89:11 ratio and 69% combined yield (see Scheme 4 and Table 3). By using the tin(II) azaenolate $SnCl^+$**12**$^-$, addition to the benzylated aldehyde (*R*,*R*)-**19a** proceeded with higher yield but almost the same stereoselectivity and gave rise to **20a** in 73% yield as a single diastereoisomer after chromatography. The additions of metalated azaenolates M^+**12**$^-$ to 2,3-*O*-isopropylidene-D-erythrose ((*R*,*R*)-**19c**) were studied next. To this end, lactol (*R*,*R*)-**19c** was slowly added to THF solution of 3 equiv of azaenolate Li^+**12**$^-$ at −78 °C, and the reaction mixture was gradually warmed to 0 °C during 12 h. After quenching, workup, and removal of the excess of (*R*)-**12**,[33] a 50:33:17 mixture of 3,6-*trans*-3,1′-*syn*-1,′2′-*anti* adduct **20c** and two other diastereoisomers was isolated in 55% yield. In contrast, when Li^+**12**$^-$ was allowed to react with stannous chloride (THF, −78 °C, 1 h) prior to the addition of lactol (*R*,*R*)-**19c**, and the reaction was performed under the same conditions (THF, from −78 to 0 °C, 12 h), **20c** was obtained in 93% as the sole aldol product (see Table 3).

Addition of 4-*O*-benzyl-2,3-*O*-isopropylidene derivative of L-erythrose (*S*,*S*)-**19a** to 1.2 equiv of the "mismatched" azaenolate Li^+**12**$^-$ at −78 °C in THF afforded, after quenching and aqueous workup, a mixture of three adducts **21a/22a/23a** in a combined yield of 60% (see Scheme 5). According to the ^{1}H NMR of the mixture the ratio between the diastereoisomers **21a/22a/23a** was 47:37:16 (see Table 4, entry 1). To evaluate the counterion dependence of the stereochemical outcome of the aldol addition, the lithium azaenolate was allowed to react with $ZnCl_2$, $SnCl_2$, $MgBr_2$·OEt_2, or $Ti(NEt_2)_3Cl$ in THF at −78 °C for 1 h, to produce the corresponding transmetalated azaenolates M^+**12**$^-$ prior to the addition of the benzylated L-erythrose acetonide. Reaction of (*S*,*S*)-**19a** with the zinc(II) azaenolate resulted in a very low conversion to products, and the mixture of adducts **21a/22a/23a**, with a 46:28:25 ratio, was obtained in 14% yield (see Table 4, entry 2). After switching the counterion of the lithium azaenolate to Sn(II), Mg(II), or Ti(IV), the aldol additions to (*S*,*S*)-**19a** led to mixtures of the same adducts **21a/22a/23a** in 60−65% yield. ^{1}H NMR analysis of these mixtures revealed slightly higher ratios of the 3,6-*trans*-3,1′-*anti*-1′,2′-*anti* diastereoisomer **21a** (see Table 4 and compare entries 3−6 with 1). In this manner, after chromatographic purification, the benzylated adducts **21a**, **22a**, and **23a** could be isolated as single diastereoisomers in yields up to 42%, 25%, and 10%, respectively.

TABLE 4. Aldol Additions of M^+12^- to L-Erythrose Acetonide (*S*,*S*)-19a

entry	(*R*)-**12** equiv	additive (equiv)	yield[a]	**21a/22a/23a** ratio[b,c]
1	1.2		60	47:37:16
2	1.2	$ZnCl_2$ (2.4)	14	46:28:25
3	1.2	$SnCl_2$ (1.2)	65	57:38:5
4	1.2	$SnCl_2$ (2.4)	65	65:31:3
5	1.2	$MgBr_2$·OEt_2 (2.4)	60	64:22:14
6	1.2	$Ti(NEt_2)_3Cl$ (1.2)	60	64:27:9

[a] Isolated yield of mixtures of diastereomeric adducts, after column chromatography. [b] Determined by integration of the ^{1}H NMR spectra of the crude mixtures. [c] Reaction conducted at −78 °C in THF.

TABLE 5. Aldol Additions of M^+12^- to L-Erythrose Acetonide (*S*,*S*)-19c

entry	(*R*)-**12** equiv	additive (equiv)	yield[a]	**21c/22c/23c** ratio[b,c]
1	3.0		52	62:38:—
2	3.0	$ZnCl_2$ (6.0)	NR[d]	
3	3.0	TMSCl + $SnCl_4$ (3.0)	NR[d]	
4	3.0	$SnCl_2$ (3.0)	78	77:3:20
5	3.0	$SnCl_2$ (6.0)	89	91:9:—
6	3.0	$Ti(O^iPr)_3Cl$ (3.0)	70	66:33:10
7	3.0	$Ti(NEt_2)_3Cl$ (3.0)	78	30:70:—
8	3.0	$MgBr_2$·OEt_2 (3.0)	70	33:6:61

[a] Isolated yield of mixtures of diastereomeric adducts, after column chromatography. [b] Determined by integration of the ^{1}H NMR spectra of the crude mixtures. [c] Reaction conducted from −78 to 0 °C in THF. [d] No reaction was observed.

When lactol (*S*,*S*)-**19c** was added to THF solutions of 3 equiv of lithium, tin(II), titanium(IV), or magnesium(II) azaenolates M^+**12**$^-$ at −78 °C and the reactions were gradually warmed to 0 °C, the aldol additions took place within 12 h. After quenching, aqueous workup, and removal of the excess of (*R*)-**12**,[33] mixtures containing up to three diastereomeric adducts **21c/22c/23c** were isolated in 52−89% yield (see Scheme 5 and Table 5). Conversely, reactions of zinc(II) azaenolate or trimethylsilylated azaenolate (promoted by $SnCl_4$) with lactol (*S*,*S*)-**19c** were not observed in the same conditions (12 h at 0 °C) or with longer reaction times and higher temperatures (see Table 5, entries 2 and 3). The stereochemical course of the azaenolate additions to the lactol (*S*,*S*)-**19c** was found to be markedly dependent on the nature of the metal salt, and thus, the three diastereoisomers, **21c**, **22c**, or **23c**, could be selectively prepared by using $SnCl^+$, $Ti(NEt_2)_3^+$, or $MgBr^+$ as counterion. Addition of the lithium azaenolate to lactol (*S*,*S*)-**19c** took place with a complete 3,6-*trans*-stereoselection and led to a 62:38 mixture of the 3,1′-

anti-1′,2′-*anti*, and 3,1′-*syn*-1′,2′-*syn* adducts, **21c** and **22c**, respectively, in 52% combined yield (see Table 5, entry 1). The *trans*,*anti*,*anti*-stereoselectivity of this aldol addition could be markedly increased by using the tin(II) azaenolate. Thus, addition of $SnCl^+$**12**$^-$ to lactol (*S*,*S*)-**19c** afforded a 77:3:20 mixture of **21c**/**22c**/**23c** in 78% combined yield (see Table 5, entry 4). We were delighted to observe that in the presence of an excess of $SnCl_2$ the reaction of $SnCl^+$**12**$^-$ with (*S*,*S*)-**19c** gave rise to a mixture of adducts **21c**/**22c** in a 91:9 ratio and 89% yield (see Table 5, entry 5).[39] In this manner, by using the tin(II) azaenolate, the 3,6-*trans*-3,1′-*anti*-1′,2′-*anti* adduct **21c** could be obtained as a single diastereoisomer in 81% yield after chromatographic purification. The stereochemical result of the aldol addition could be further modulated by tuning the ligands of the titanium(IV) azaenolate. In the presence of $Ti(O^iPr)_3Cl$ there was not significant change in the yield nor the stereoselectivity of the reaction of the lithium azaenolate with the lactol (see Table 5, entries 1 and 6), whereas when using $Ti(NEt_2)_3Cl$ as additive, the same aldol addition proceeded with the opposite selectivity. Thus, reaction of $Ti(NEt_2)_3^+$**12**$^-$ with lactol (*S*,*S*)-**19c** was found to be *trans*,*syn*,*syn*-selective and gave rise to a 30:70 mixture of adducts **21c**/**22c** in 78% combined yield (see Table 5, entry 7). In this case, the 3,6-*trans*-3,1′-*syn*-1′,2′-*syn* adduct **22c** could be obtained as a single diastereoisomer in 54% yield after chromatographic purification. Finally, switching the metal of the azaenolate to magnesium drastically changed the stereochemical outcome of the addition to the lactol, which took place with a moderate *cis*-selectivity. Thus, reaction of $MgBr^+$**12**$^-$ with (*S*,*S*)-**19c** furnished a mixture of adducts **21c**/**22c**/**23c** in a 33:6:61 ratio and 70% combined yield (see Table 5, entry 8). Formation of the 3,6-*cis*-3,1′-*syn*-1′,2′-*anti* diastereoisomer **23c** as the major aldol addition product was surprising, as there was not any precedent for such *cis*-selective addition in the Schöllkopf's bislactim chemistry.[40]

The observation of remarkable *trans*,*anti*,*anti*-selectivity in the addition of azaenolate $SnCl^+$**12**$^-$ to the erythrose acetonide (*S*,*S*)-**19c** stands in contrast to the *trans*,*syn*,*syn*-selectivity seen for the additions of $SnCl^+$**15**$^-$ to threose acetonides **13a,b** (see Table 2) or other mismatched α-alkoxyaldehydes.[29] To account for the striking effect of the free hydroxyl group at the acceptor in the stereochemical outcome of the aldol addition, we initially postulated a change of the reaction mechanism to a reversible one. To address this possibility we subjected a 62:38 mixture of adducts **21c**/**22c** (prepared by reaction of Li^+**12**$^-$ with (*S*,*S*)-**19c**; see entry 1 of Table 5) to reaction with 4 equiv of tin(II) azaenolate $SnCl^+$**12**$^-$. The reversibility of the aldol addition would enforce the enrichment of the mixture of adducts in the *trans*,*anti*,*anti*-diastereoisomer. Nevertheless, after a prolonged reaction time at 0 °C, quenching, workup, and removal of the excess of (*R*)-**12**, the ratio between the diastereoisomers **21c**/**22c** was unchanged, ruling out the involvement of the postulated equilibrium between the aldolates in the presence of tin(II) salts. Additional information supporting the non-involvement of equilibrium between the tin(II) aldolates was provided by determination of the same ratio between diastereoisomers **21c**/**22c** (91:9) in the aliquots retrieved at different temperatures (−30, −20, −10, and 0 °C) from the reaction mixture of $SnCl^+$**12**$^-$ and (*S*,*S*)-**19c**.

Evidence supporting the relative configuration of all aldol adducts was obtained from NMR analyses and chemical correlation. For the 3,6-*trans* diastereoisomers (**14a**−**c**, **16a**−**c**, **17a**−**c**, **20a,c**, **21a,c**, and **22a,c**) the H-6 resonance appears between 3.91 and 4.02 ppm, as a triplet with ^5J(H3,H6) close to 3.5 Hz, which is general of the *trans* relationship of substituents at the pyrazine ring. Conversely, the ^{1}H NMR spectrum of adduct **23a** shows the absorption corresponding to H-6 at 3.88 ppm, as a doublet of doublets with a ^5J(H3,H6) of 5.9 Hz, which is typical of a 3,6-*cis* relationship at the bislactim ether ring.[41] Furthermore, the configurations of all the adducts were unambiguously confirmed through their conversion into known piperidine alkaloids. Thus, the adducts **14a**−**c**, **16a**−**c**, and **17a**−**c**, derived from L-threose, were transformed into 1-deoxy-D-galactonojirimycin, 1-deoxy-L-idonojirimycin, and 1-deoxy-L-altronojirimycin, respectively, and the adducts **20a,c**, **21a,c**, **22a,c**, and **23a,c**, derived from erythrose, were used in the preparation of 1-deoxy-D-talonojirimycin, 1-deoxy-D-allonojirimycin, 1-deoxy-D-gulonojirimycin and 1-deoxy-L-talonojirimycin, respectively, as will be described below (see Schemes 12 and 14).

2. Models for Diastereoselective Aldol Additions with Tin(II) Salts of Bislactim Ethers. The stereoselectivities of the aldol additions of metalated bislactim ethers to a variety of aldehydes have been rationalized with the Zimmerman−Traxler six-membered ring model.[42] Reaction of the metalated bislactim ether by its less-hindered side, opposite to the isopropyl group, through a chair-like transition-state structure (TS) with an equatorial disposition of the aldehyde (see **Ce** in Scheme 6) should be favored and can account for the formation of the major 3,6-*trans*-3,1′-*syn* addition product. The 3,6-*trans*-3,1′-*anti* minor product could arise from a switch to an axial disposition of the aldehyde moiety in the chair-like TS (**Ca**) or from involvement of boat-like TS (**Be**) with less serious diaxial interactions.

Matched and mismatched situations arise in the reaction of metalated bislactim ethers and chiral aldehydes. To explain the high stereoselection in the additions of metalated bislactim ethers to matched α-alkoxyaldehydes, the pericyclic TS has been combined with the Felkin−Anh model[43] or the modified Cornforth model[44] for 1,2-asymmetric induction. Thus, Schöllkopf postulated the involvement of chair-Felkin-Anh TS (like **F**, see Scheme 7), stabilized through hyperconjugative interaction of the forming bond (HOMO) with the α-alkoxy bond (LUMO), to account for the almost exclusive formation of 3,6-*trans*-3,1′-*syn*-1′,2′-*anti* adduct.[28a] Nevertheless, TS **F** should be destabilized by the presence of a double gauche pentane interaction[44,45] between one nitrogen atom of the bislactim and the carbon chain

(39) Improved diastereoselectivities and yields by using 2 equiv of metal salts were also reported in the aldol reactions of other amino ester enolates; see: Kazmaier, U.; Grandel, R. *Synlett* **1995**, 945−946.

(40) Protonation of potassium azaenolates derived from *cyclo*-[L-Val-Ala] with acetic acid has been reported as *cis*-selective; see: Hünig, S.; Klaunzer, N.; Wenner, H. *Chem. Ber.* **1994**, *127*, 165−172.

(41) See, for instance: (a) Busch, K.; Groth, U. M.; Kühnle, W.; Schöllkopf, U. *Tetrahedron* **1992**, *48*, 5607−5618. (b) Ruiz, M.; Fernández, M. C.; Díaz, A.; Quintela, J. M.; Ojea, V. *J. Org. Chem.* **2003**, *68*, 7634−7645. (c) Fernández, M. C.; Díaz, A.; Guillín, J. J.; Blanco, O.; Ruiz, M.; Ojea, V. *J. Org. Chem.* **2006**, *71*, 6958−6974.

(42) (a) Evans, D. A.; Nelson, J. V.; Taber, T. R. *Top. Stereochem.* **1982**, *13*, 1−115. (b) Zimmerman, H. E.; Traxler, M. D. *J. Am. Chem. Soc.* **1957**, *79*, 1920−1923.

(43) (a) Anh, N. T. *Top. Curr. Chem.* **1980**, *88*, 145−162. (b) Anh, N. T.; Eisenstein, O. *Nouv. J. Chim.* **1977**, *1*, 61−70. (c) Chérest, M.; Felkin, H.; Prudent, N. *Tetrahedron Lett.* **1968**, 2199−2204.

(44) (a) Evans, D. A.; Cee, V. J.; Siska, S. J. *J. Am. Chem. Soc.* **2006**, *128*, 9433−9441. (b) Evans, D. A.; Siska, S. J.; Cee, V. J. *Angew. Chem., Int. Ed.* **2003**, *42*, 1761−1765.

(45) Roush, W. R. *J. Org. Chem.* **1991**, *56*, 4151−4157 and references therein.

SCHEME 6

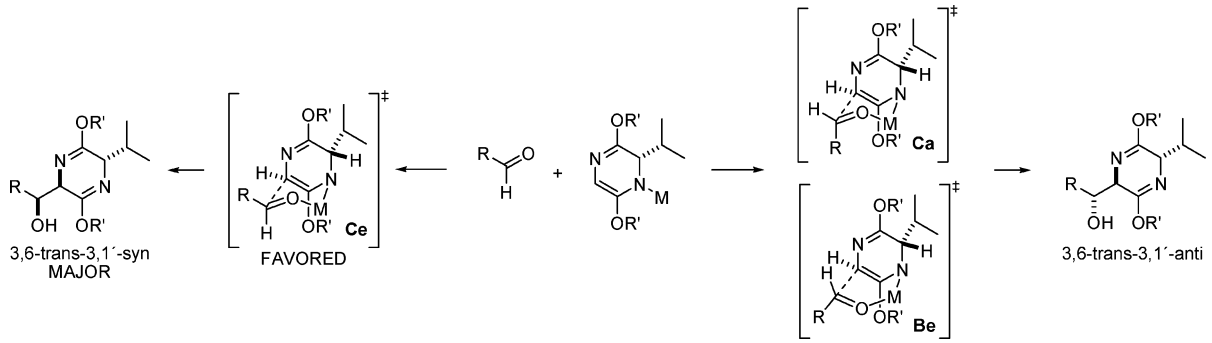

SCHEME 7

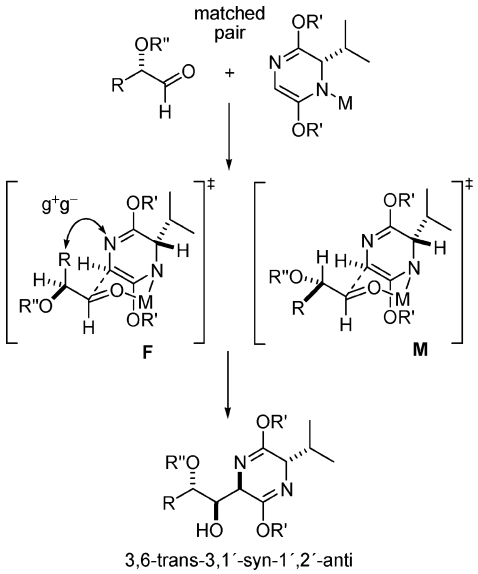

of the aldehyde. This unfavorable steric interaction raises the energy of the Felkin−Anh pathway, and other transition-state structures (TSs) that minimize all nonbonded interactions may become lower in energy. According to our ab initio calculations, the Cornforth-like TS (**M**, see Scheme 7), minimizing both the gauche interactions and the dipole interaction between the α-alkoxy and carbonyl group, resulted as the preferred one in the addition of lithiated bislactim ethers to matched glyceraldehyde-derived acetonides.[25d]

Highly diastereoselective aldol reactions using chiral tin(II) enolates have been successfully applied in asymmetric synthesis.[46] In the present article we have shown that the aldol additions of bislactim ethers to erythrose or threose acetonides take place with the highest stereoselectivity when using tin(II) azaenolates. The stereochemical outcome for such tin(II)-mediated aldol reactions has been qualitatively rationalized in terms of tightly chelated chair-like TSs. Nevertheless, compared to other metal enolates, the tin−oxygen bond in tin(II) enolates is not relatively short and does not necessarily lead to tighter cyclic TSs nor higher levels of stereoselectivity. Although numerous theoretical investigations have shed light on the TSs for aldol additions using different metal enolates,[47] the proposed models for the tin(II)-mediated aldol reactions have not been supported by subsequent computational studies. We analyze herein the extension of these models to the reaction of tin(II) azaenolates with matched and mismatched acetonides derived from glyceraldehyde or erythrose and show that DFT calculations provide valuable insight to rationalize the experimental diastereoselectivity. To this end, geometry optimizations were performed using a B3LYP DFT procedure[48] with the cc-pVDZ basis set[49] and a small-core relativistic pseudopotential (PP) for Sn.[50] Single-point energy calculations were performed at the B3LYP/cc-pVTZ-PP level (see Computational Methods in Supporting Information).

2.1. Tin(II) Azaenolate/Lithium Chloride Aggregates. We first studied the reaction of lithium azaenolate derived from (*R*)-**15** with tin(II) chloride and three molecules of THF in the gas phase (see Scheme 8). Formation of unsolvated tin(II) azaenolate **uA** and trisolvated lithium chloride was calculated to be exothermic by more than 16 kcal/mol, and dimerization of **uA** was endothermic (see Supporting Information, Scheme S1). Conversely, association of **uA** and the lithium chloride generated in situ to give a disolvated mixed aggregate **dA** was favored by more than 13 kcal/mol. Most stable mixed aggregate was

(46) (a) Gridley, J. J.; Coogan, M. P.; Knight, D. W.; Malik, K. M. A.; Sharland, C. M.; Singkhonrat, J.; Williams, S. *Chem. Commun.* **2003**, 2550−2551. (b) Matsui, K.; Zheng, B.-Z.; Kusaka, S.-i.; Kuroda, M.; Yoshimoto, K.; Yamada, H.; Yonemitsu, O. *Eur. J. Org. Chem.* **2001**, 3615−3624. (c) Franck-Neumann; Miesch-Gross, L.; Gateau, C. *Eur. J. Org. Chem.* **2000**, 3693−3702. (d) Sano, S.; Ishii, T.; Miwa, T.; Nagao, Y. *Tetrahedron Lett.* **1999**, *40*, 3013−3016. (e) Paterson, I.; Franklin, A. S. *Tetrahedron Lett.* **1994**, *35*, 6925−6928. (f) Pridgen, L. N.; Abdel-Magid, A. F.; Lantos, I.; Shilcrat, S.; Eggleston, D. S. *J. Org. Chem.* **1993**, *58*, 5107−5117. (g) Nagao, Y.; Nagase, Y.; Kumagai, T.; Matsunaga, H.; Abe, T.; Shimada, O.; Hayashi, T.; Inoue, Y. *J. Org. Chem.* **1992**, *57*, 4243−4249. (h) Paterson, I.; Tillyer, R. D. *Tetrahedron Lett.* **1992**, *33*, 4233−4236. (i) Bodwell, G. J.; Davies, S. G.; Mortlock, A. A. *Tetrahedron* **1991**, *47*, 10077−10086. (j) Evans, D. A.; Clark, J. S.; Metternich, R.; Novack, V. J.; Sheppard, G. S. *J. Am. Chem. Soc.* **1990**, *112*, 866−868. See also ref 29b.

(47) Lithium enolates: (a) Pratt, L. M.; Nguyen, N. V.; Ramachandran, R. *J. Org. Chem.* **2005**, *70*, 4279−4283. (b) Abu-Hasanayn, F.; Streitwieser, A. *J. Org. Chem.* **1998**, *63*, 2954−2960. (c) Henderson, K. W.; Dorigo, A. E.; Liu, Q.-Y.; Williard, P. G.; Schleyer, P. v. R.; Bernstein, P. R. *J. Am. Chem. Soc.* **1996**, *118*, 1339−1347. (d) Bernardi, F.; Bongini, A.; Cainelli, G.; Robb, M. A.; Valli, G. S. *J. Org. Chem.* **1993**, *58*, 750−755. (e) Leung-Tong, R.; Tidwell, T. T. *J. Am. Chem. Soc.* **1990**, *112*, 1042−1048. (f) Li, Y.; Paddon-Row, M. N.; Houk, K. N. *J. Org. Chem.* **1990**, *55*, 481−493 and references therein. Boron enolates: (g) Goodman, J. M.; Paton, R. S. *Chem. Commun.* **2007**, 2124−2126 and references therein. (h) Cee, V. J.; Cramer, C. J.; Evans, D. A. *J. Am. Chem. Soc.* **2006**, *128*, 2920−2930. (i) Murga, J. Falomir, E.; Gonzalez, F.; Carda, M.; Marco, J. A. *Tetrahedron* **2002**, *58*, 9697−9707. Silicon enolates: (j) Wong, C. T.; Wong, M. W. *J. Org. Chem.* **2007**, *72*, 1425−1430. (k) Denmark, S. E.; Fan, Y.; Eastgate, M. D. *J. Org. Chem.* **2005**, *70*, 5235−5248. (l) Silva López, C.; Álvarez, R.; Vaz, B.; Nieto Faza, O.; de Lera, A. R. *J. Org. Chem.* **2005**, *70*, 3654−3659. Titanium enolates: (m) Itoh, Y.; Yamanaka, M.; Mikami, K. *J. Am. Chem. Soc.* **2004**, *126*, 13174−13175. Tin(IV) enolates: (n) Yasuda, M.; Chiba, K.; Baba, A. *J. Am. Chem. Soc.* **2000**, *122*, 7549−7555.

(48) (a) Becke, A. D. *J. Chem. Phys.* **1993**, *98*, 5648−5652. (b) Lee, C.; Yang, W.; Parr, R. G. *Phys. Rev. B* **1988**, *37*, 785−789.

(49) (a) Davidson, E. R. *Chem. Phys. Lett.* **1996**, *260*, 514−518. (b) Woon, D. E.; Dunning, T. H., Jr. *J. Chem. Phys.* **1993**, *98*, 1358−1371. (c) Dunning, T. H., Jr. *J. Chem. Phys.* **1989**, *90*, 1007−1023.

(50) Peterson, K. A. *J. Chem. Phys.* **2003**, *119*, 11099−11112.

SCHEME 8

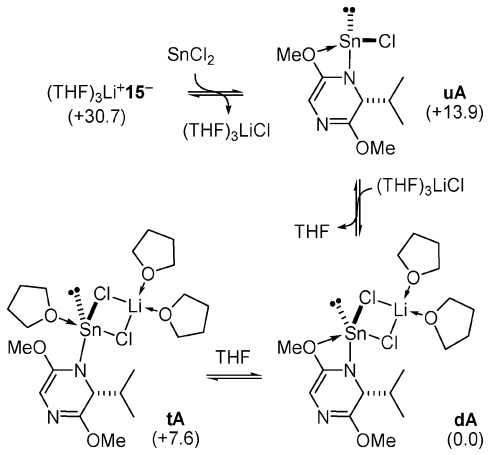

SCHEME 9

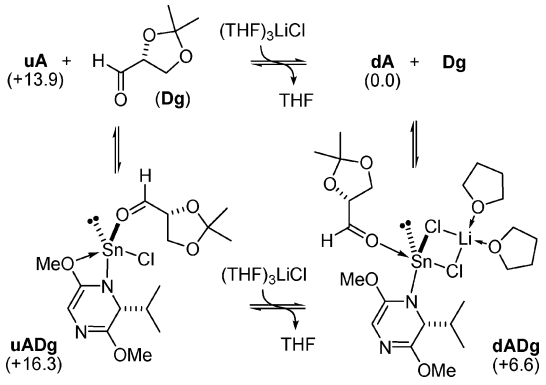

characterized by a tetrahedral environment for the lithium cation due to contacts with two chlorides and two THF molecules and a distorted trigonal-bipyramidal geometry about the tin(II) cation with anticlockwise (*A*) configuration. In the mixed aggregate the azaenolate coordinates to the tin(II) cation in a bidentate fashion, with the anionic nitrogen occupying an equatorial position and the vicinal methoxy group located at an axial site. In addition, one chloride is located axially while the second chloride and the lone pair of electrons occupy the remaining equatorial sites of the tin(II) cation. Binding of a third THF molecule to **dA** to give the trisolvated mixed aggregate **tA** was found to be endothermic by more than 7 kcal/mol (see Supporting Information, Table S1). The aggregation of a tin(II) enolate in the solid state has been previously reported.[51]

2.2. Models for the Addition of Tin(II) Azaenolate to Glyceraldehyde Acetonides. The aldol reactions of D-glyceraldehyde acetonide (**Dg**) with azaenolates **uA** or **dA** proceed first by the endothermic formation of the intermediate complexes **uADg** and **dADg**, respectively (see Scheme 9). Both intermediate complexes maintain the distorted trigonal-bipyramidal environment for the tin(II) cation with *A* configuration. While the unsolvated complex **uADg** is characterized by the contact between the vicinal methoxy group and the tin(II) cation, this interaction is not present in the disolvated complex **dADg**. Most stable unsolvated complex **uADg** showed both the azaenolate nitrogen and the aldehyde ligands located at equatorial sites about the tin(II) cation. Conversely, most stable disolvated complex **dADg** showed the aldehyde ligand placed in an axial location and the azaenolate nitrogen occupying an equatorial site. Association of **uADg** to lithium chloride and two THF molecules to form **dADg** was favored by more than 9 kcal/mol in the gas phase. Because separate disolvated azaenolate and glyceraldehyde acetonide (**dA** + **Dg**) was the most stable state for reactants, it was used as the reference for calculation of the activation barriers.

The possible pathways for the reorganization of the intermediate complexes **uADg** and **dADg** were analyzed next. Pericyclic TSs connecting these intermediates to the corresponding unsolvated or disolvated aldolates with either 3,6-*cis*-3,1′-*anti*-1′,2′-*anti*, 3,6-*cis*-3,1′-*syn*-1′,2′-*syn*, 3,6-*trans*-3,1′-*anti*-1′,2′-*syn*, or 3,6-*trans*-3,1′-*syn*-1′,2′-*anti* configuration were grouped into four diastereomeric pathways that were designated as **caa**, **css**, **tas**, and **tsa**, respectively. In each diastereomeric pathway, different starting geometries were subjected to optimization considering the following main structural features: (1) boat-like and chair-like conformations for the pericyclic ring (denoted "B" and "C", respectively), (2) three different trigonal-bipyramidal environments for the tin(II) cation, with equatorial aldehyde-equatorial azaenolate, equatorial aldehyde-axial azaenolate, or axial aldehyde-equatorial azaenolate (denoted "ee", "ea", and "ae", respectively), and (3) Felkin−Anh, Cornforth, and non-Anh[52] conformations (denoted "F", "M" and "N", respectively) for the aldehyde moiety (see Supporting Information, Figure S1). In addition, clockwise and anticlockwise configurations for the trigonal-bipyramidal tin(II) cation were constructed for all the selected geometries. Representative starting geometries for TS location are depicted in Figure S2 of the Supporting Information.

For a rapid computation of the stereoselectivity of the aldol addition we first studied the TSs arising from the reorganization of the unsolvated intermediate complex **uADg**. Most stable unsolvated TSs lay in almost the same position along the reaction coordinate (with C−C bond forming distance between 2.36 and 2.45 Å) and are characterized by a distorted tetrahedral environment for tin(II) cation, due to contacts with the chloride, the aldehyde oxygen, and the azaenolate nitrogen (see Figure 1 and Figure S3 of the Supporting Information). Thus, the coordination between the tin(II) cation and the vicinal methoxy group, which was present in the parent complex **uADg**, was not maintained in the unsolvated TSs. In all the diastereomeric pathways, TSs with *S* configuration at the metal center showed energy values lower than those of their epimers with *R* configuration. In agreement with the experimental results, the most favorable unsolvated TS was located in the *trans*,*syn*,*anti* diastereomeric pathway. This TS, designated as **utsa**-CM, was characterized by chair-like and Cornforth-like conformations for the pericyclic ring and the aldehyde moiety, respectively (see Figure 1). In the *trans*,*anti*,*syn* diastereomeric pathway the most favorable TS was **utas**-BN, which showed boat-like and non-Anh conformations and was only 0.8 kcal/mol higher in energy than **utsa**-CM. The competitive unsolvated TSs in the *cis*,*anti*,*anti* and *cis*,*syn*,*syn* pathways were computed to be more than 13 kcal/mol higher in energy (see Figure S3 and Table S2 of the Supporting Information). Assuming a Boltzmann distribution of the unsolvated TSs at −78 °C, the calculated *trans*,*syn*,*anti*/

(51) Driess, M.; Dona, N.; Merz, K. *Chem. Eur. J.* **2004**, *10*, 5971−5976.

(52) The term "non-Anh" was coined by Heathcock to designate the reactive conformations having one of the ligands on the stereogenic α-carbon with higher σ* orbital energy *anti* to the incoming nucleophile. See: (a) Lodge, E. P.; Heathcock, C. H. *J. Am. Chem. Soc.* **1987**, *109*, 3353−3361. (b) Gawley, R. E.; Aubé, J. *Principles of Asymmetric Synthesis*; Pergamon: New York 1996; pp 127−130.

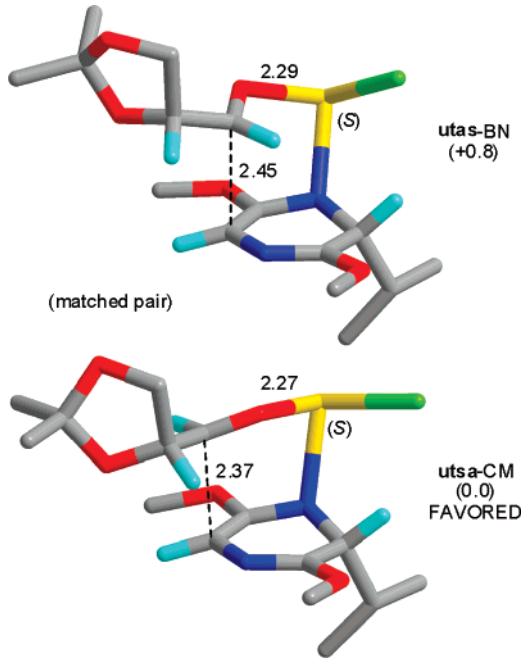

FIGURE 1. Chem3D representations of the most favored unsolvated TSs located (B3LYP/cc-pVDZ-PP level) for the aldol addition of unsolvated tin(II) azaenolate (**uA**) to D-glyceraldehyde acetonide (**Dg**). Relative energies in the gas phase (B3LYP/cc-pVTZ-PP level) are shown in parenthesis in kcal/mol. Distances are in angstroms. The hydrogen atoms are omitted for clarity except at chiral and reaction centers. Legend: carbon = gray, nitrogen = blue, oxygen = red, hydrogen = turquoise, tin = yellow, chlorine = green.

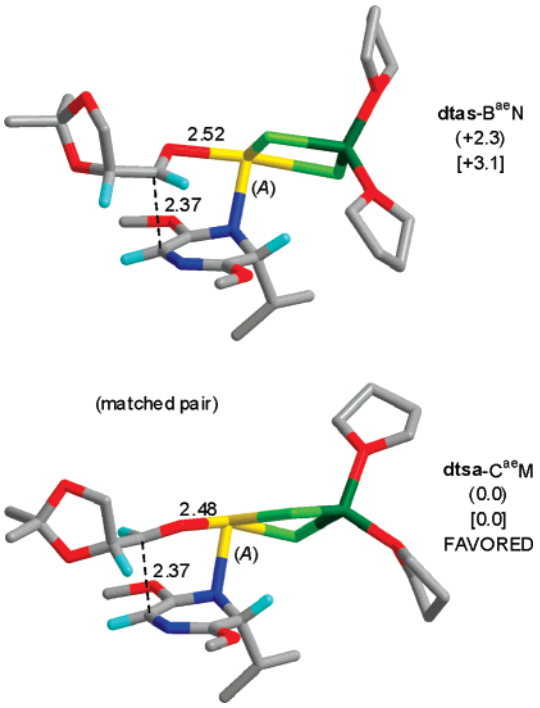

FIGURE 2. Chem3D representations of the most favored disolvated TSs located (B3LYP/cc-pVDZ-PP level) for the aldol addition of disolvated tin(II) azaenolate (**dA**) to L-glyceraldehyde acetonide (**Dg**). Relative energies in the gas phase (B3LYP/cc-pVTZ-PP level) and in THF solution (B3LYP(SCRF)/cc-pVTZ-PP level using the PCM method) are shown in parenthesis and brackets, respectively (kcal/mol). Distances are in angstroms. The hydrogen atoms are omitted for clarity except at chiral and reaction centers. Legend: carbon = gray, nitrogen = blue, oxygen = red, hydrogen = turquoise, tin = yellow, chlorine = light green, lithium = green.

trans,anti,syn ratio (ca. 9:1) was lower than the experimental trend (see Tables 1 and 3 and ref 29a,c). In this manner, unsolvated models were very much simplified and reproduced the sense but not the degree of the stereoselection in the aldol additions of tin(II) azaenolates to matched acetonides derived from glyceraldehyde.

To further optimize our computational model, we undertake the study of the TSs arising from the disolvated mixed aggregate **dADg**, which demanded a higher computational effort. All optimized disolvated TSs were characterized by a distorted trigonal-bipyramidal geometry about the tin(II) cation. In all diastereomeric pathways, the most stable TSs showed almost the same C−C bond-forming distances (between 2.37 and 2.45 Å) and were characterized by *A* configurations around the tin(II) cation, with the aldehyde and the azaenolate moieties located at axial and equatorial sites, respectively (see Figure 2 and Figure S4 of the Supporting Information). Axial bond lengths at the tetracoordinate tin(II) cation of the mixed aggregates were distinctly longer than for the three-coordinate metal of the unsolvated TSs (average differences are 0.24 Å for Sn−O). In the gas phase, disolvated TS **dtsa**-C^{ae}M, with a chair-like conformation for the pericyclic ring and a Cornforth-like conformation for the aldehyde moiety was computed as the lowest in energy. This *trans,syn,anti* TS was favored by 2.3 kcal/mol over the corresponding most favorable *trans,anti,syn* TS, which showed boat and non-Anh conformations for the pericyclic ring and the aldehyde moiety (see **dtas**-B^{ae}N in Figure 2). As previously found in the unsolvated reaction channel, the disolvated TSs in the *cis* pathways were computed to be more than 12 kcal/mol higher in energy (see **dcaa**-C^{ae}M and **dcss**-C^{ae}F in Figure S4 and Table S3 of the Supporting Information). According to the calculations, the free energy barriers for the disolvated TSs **dtsa**-C^{ae}M and **dtas**-B^{ae}N were more than 4 kcal/mol lower than those previously computed for the most favorable unsolvated TSs (see Table 6). In this manner, the mixed aggregates offered the lowest energy channel for the aldol reaction. Moreover, the energy gap between **dtsa**-C^{ae}M and the competing TSs is consistent with the high diastereofacial bias observed in the additions of tin(II) azaenolates to matched acetonides derived from threose and erythrose.

TABLE 6. Relative Energies and Energy Barriers for TSs Located in the Addition of Tin(II) Azaenolates to Glyceraldehyde Acetonides

	gas phase		THF	
model (*config*)	rel E^a (kcal/mol)	$\Delta G^{\ddagger 195\,a}$ (kcal/mol)	rel E^e (kcal/mol)	$\Delta G^{\ddagger 195\,e}$ (kcal/mol)
utsa-CM(*S*)	0.0	17.7[b]		
utas-BN(*S*)	0.8	18.0[b]		
dtsa-C^{ae}M(*A*)	0.0	11.1[c]	0.0	15.4[c]
dtas-B^{ae}N(*A*)	2.3	13.4[c]	3.1	18.5[c]
dtas-C^{ae}N(*A*)	4.7	15.8[c]	2.3	17.7[c]
dtaa-C^{ae}M(*A*)	0.0	13.2[d]	0.0	15.4[d]
dtss-C^{ae}F(*A*)	1.8	15.0[d]	1.4	16.8[d]

[a] Calculated at the B3LYP/cc-pVTZ-PP//B3LYP/cc-pVDZ-PP level. [b] Free activation energy (195 K, 1 atm) relative to **dA**+**Dg**+THF-(THF)$_3$LiCl. [c] Free activation energy (195 K, 1 atm) relative to **dA**+**Dg**. [d] Free activation energy (195 K, 1 atm) relative to **dA**+**Lg**. [e] Calculated at B3LYP(SCRF)/cc-pVTZ-PP//B3LYP(SCRF)/cc-pVDZ-PP level using the PCM method.

Following the same strategy for the study of the reaction between the disolvated tin(II) azaenolate **dA** and the mismatched L-glyceraldehyde acetonide (**Lg**), similar results were obtained.

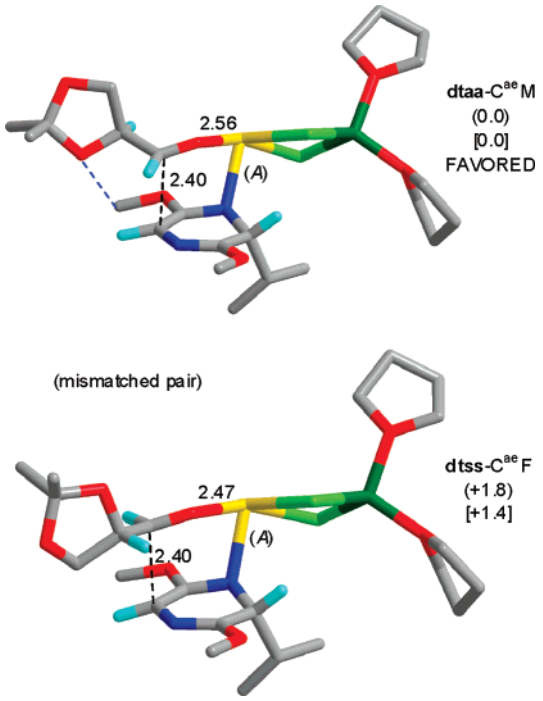

FIGURE 3. Chem3D representations of the most favored disolvated TSs located (B3LYP/cc-pVDZ-PP level) for the aldol addition of disolvated tin(II) azaenolate (**dA**) to L-glyceraldehyde acetonide (**Lg**). Relative energies in the gas phase (B3LYP/cc-pVTZ-PP level) and in THF solution (B3LYP(SCRF)/cc-pVTZ-PP level using the PCM method) are shown in parenthesis and brackets, respectively (kcal/mol). Distances are in angstroms. The hydrogen atoms are omitted for clarity except at chiral and reaction centers. Legend: carbon = gray, nitrogen = blue, oxygen = red, hydrogen = turquoise, tin = yellow, chlorine = light green, lithium = green.

Full optimization of the selected geometries for the intermediate complex **dALg** enabled the location of the corresponding TSs in the 3,6-*cis*-3,1′-*anti*-2′,3′-*syn*, 3,6-*cis*-3,1′-*syn*-2′,3′-*anti*, 3,6-*trans*-3,1′-*anti*-2′,3′-*anti*, and 3,6-*trans*-3,1′-*syn*-2′,3′-*syn* diastereomeric pathways, which were designated as **cas**, **csa**, **taa**, and **tss**. As previously found for the matched situation, the most favorable mismatched TSs were characterized by almost the same C−C bond-forming distances (between 2.36 and 2.40 Å) and *A* configurations around the trigonal-bipyramidal tin(II) cation, with the aldehyde-azaenolate pair of ligands placed at axial−equatorial sites. The mismatched TS of lowest energy was found in the *trans*,*anti*,*anti* diastereomeric pathway. Here again, most stable TS showed a chair-like conformation for the pericyclic ring and a Cornforth-like conformation for the aldehyde moiety (see **dtaa**-C^{ae}M in Figure 3). Most favored TS in the *trans*,*syn*,*syn* pathway was computed to be 1.8 kcal/mol higher in energy and showed a chair-like conformation for the pericyclic ring and a Felkin−Anh conformation for the aldehyde moiety (see **dtss**-C^{ae}F in Figure 3), while the TSs in the *cis* pathways were more than 9 kcal/mol higher in energy (see **dcas**-B^{ae}F and **dcsa**-C^{ae}M in Figure S5 and Table S4 of the Supporting Information). It should be noted that in **dtaa**-C^{ae}M the glyceraldehyde moiety is placed in an axial environment of the pericyclic ring and thus maintains a 1,3-diaxial interaction with a methoxy group of the bislactim moiety. With this 1,3-diaxial relationship, the distance between the oxygen atom at α-position of the glyceraldehyde moiety and one of the methoxy hydrogens of the bislactim was reduced to 2.35 Å, which indicated a hydrogen bond interaction. This interaction was not present in the competing TSs and therefore could contribute to the energy difference between the *trans*,*anti*,*anti* and *trans*,*syn*,*syn* pathways.[53]

To further study the influence of the solvent in the reaction path, the geometries of the most significant disolvated TSs as calculated in the gas phase were reoptimized in THF solution using the PCM method.[54] The effect of the dielectric medium simulating THF on the structures of the TSs was almost negligible. Nevertheless, nonspecific solvation of the disolvated TSs (with less charge-localized geometries) was less exothermic than that for the reactive precursors, and thus, the free energy barriers in solution were increased by 1.8−4.3 kcal/mol with respect to those calculated in the gas phase. Differential nonspecific solvation effects on the competitive TSs were rather small in both the matched and the mismatched situations. In THF solution the calculated stereoselectivity was maintained for the matched pair, while the energy gap between the mismatched TSs was reduced to 1.4 kcal/mol (see Table 6 and Table S5 in the Supporting Information).

According to DFT computations for the reaction of tin(II) azaenolate with glyceraldehyde acetonides, the *trans*,*syn*,*anti* TS is favored for the matched pair and the *trans*,*anti*,*anti* TS is favored for the mismatched one, and the calculated energy gap between the competing TSs is greater for the matched situation than for the mismatched one. Nevertheless, the asymmetric induction computed for the reaction of the tin(II) azaenolate with the mismatched glyceraldehyde model deviates from that experimentally observed in the additions to mismatched threose and erythrose acetonides. Thus, the *trans*,*anti*,*anti*/*trans*,*syn*,*syn* ratio calculated for the mismatched glyceraldehyde model (ca. 9:1, assuming a Boltzmann distribution of the TSs at −78 °C) is considerable higher than the experimental values observed for the mismatched erythrose acetonide **19a** (ca. 2:1) and even opposite in direction to that obtained with the mismatched threose acetonides **13a,b** (ca. 1:2). Thus, the results of calculations with the glyceraldehyde model can be easily extrapolated to the analysis of the additions to matched threose and erythrose acetonides. On the other hand, the differences between the stereoselectivity computed for glyceraldehyde model and experimentally observed for threose and erythrose acetonides may uncover the influence of the β-stereocenter as a third stereochemical determinant of the aldol addition. In this manner, we speculate that nonbonding interactions between the tin(II) azaenolate and the β-alkoxymethyl moiety of the threose and erythrose acetonides may result in a closer energy for the mismatched TSs and account for the reduced *trans*,*anti*,*anti*/*trans*,*syn*,*syn* ratio.

In summary, modeling studies provided some valuable insight to rationalize the stereochemical outcome for the aldol additions of tin(II) azaenolates to threose and erythrose acetonides. Calculation suggests that the experimentally observed stereoselectivity can be accounted for with a mechanism that involves a kinetically controlled reaction featuring the solvated aggregates of the tin(II) azaenolate and the lithium chloride generated in situ as the reactive species. In these solvated aggregates the tin(II) cation adopts a trigonal-bipyramidal environment in which the aldehyde-azaenolate pair of ligands are preferentially located

(53) A stabilizing hydrogen bond has been previously proposed to rationalize the stereoselectivity observed in aldol additions. See: Paton, R. S.; Goodman, J. M. *Org. Lett.* **2006**, *8*, 4299−4302 and references therein.

(54) (a) Cossi, M.; Scalmani, G.; Rega, N.; Barone, V. *J. Chem. Phys.* **2002**, *117*, 43−54. (b) Mennucci, B.; Tomasi, J. *J. Chem. Phys.* **1997**, *106*, 5151−5158.

SCHEME 10

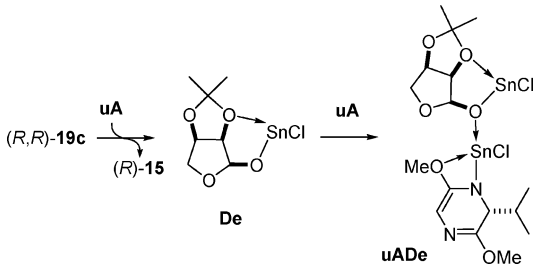

at axial−equatorial sites. For the reorganization of the solvated aggregates, the chair-like TSs with Cornforth-like conformation for the aldehyde moiety are clearly favored for both the matched and the mismatched pairs.

2.3. Models for the Addition of Tin(II) Azaenolate to Erythrose Acetonides. Reaction of tin(II) azaenolate **uA** as a base with D-erythrose acetonide (*R*,*R*)-**19c** to give bislactim ether (*R*)-**15** and tin(II) alkoxy-derivative **De** was calculated to be exothermic by more than 23 kcal/mol in the gas phase (see Scheme 10). The most stable tin(II) alkoxy-derivative from D-erythrose showed a hemiacetalic structure, with the tin(II) cation chelated by the oxygen atoms at the anomeric and α positions. Other five- and seven-membered chelate structures for the tin(II) alkoxy-derivative, showing contacts of the tin(II) cation with the oxygen atoms at *β*- and *γ*-positions (**De**-5) or at the carbonyl group and the *γ*-position (**De**-7) were higher in energy (see Scheme S2 of the Supporting Information). Addition of azaenolate **uA** to the tin(II) alkoxy-derivative **De** proceeds by the exothermic formation of the intermediate complex **uADe**, which was used as the reference for calculation of the activation barriers. Reorganization of this complex to the four possible aldolates through the **caa**, **css**, **tas**, and **tsa** diastereomeric pathways was studied next. Different geometries for **uADe** were selected for construction and optimization of the TSs, as depicted in Scheme S2 of the Supporting Information. We considered five- and seven-membered chelate rings for the erythrose moiety (denoted "5" and "7", respectively), as the lower stability of such chelates for the intermediates does not necessarily hold for the TSs where the carbonyl moiety is geometrically distorted and other steric interactions come into play. The coordination of the tin(II) cation of the azaenolate with either the oxygen at the carbonyl group or the oxygen at *γ*-position of the erythrose moiety (denoted "c" and "g", respectively) were also considered.[55] In addition, starting geometries characterized by chair-like or boat-like conformations for the pericyclic ring (denoted as "C" and "B", respectively) were subjected to optimization in each of the diastereomeric pathways.

In the gas phase, the most stable TS for reaction **uA** and **De** was located in the *trans*,*syn*,*anti* pathway, 12.8 kcal/mol above the intermediate complex **uADe**. This TS, designated as **utsa**-B7cg (see Figure 4) was characterized by a 4,6,7 ring system. One of the tin(II) cations showed a trigonal-bipyramidal environment because of the interaction with the nitrogen of the azaenolate, a chloride and the oxygens of the carbonyl and alkoxy groups of the erythrose moiety. Here again, the aldehyde-azaenolate pair of ligands were located in axial−equatorial sites around the tin(II) cation, which showed an *A* configuration. In

(55) TSs in which the tin(II) cation of the azaenolate binds to the chlorine atom of the tin(II) alkoxy-derivative of erythrose were also located (see **utas**-C7 in the Table S6 and **utaa**-B7 in the Table S7 of the Supporting Information).

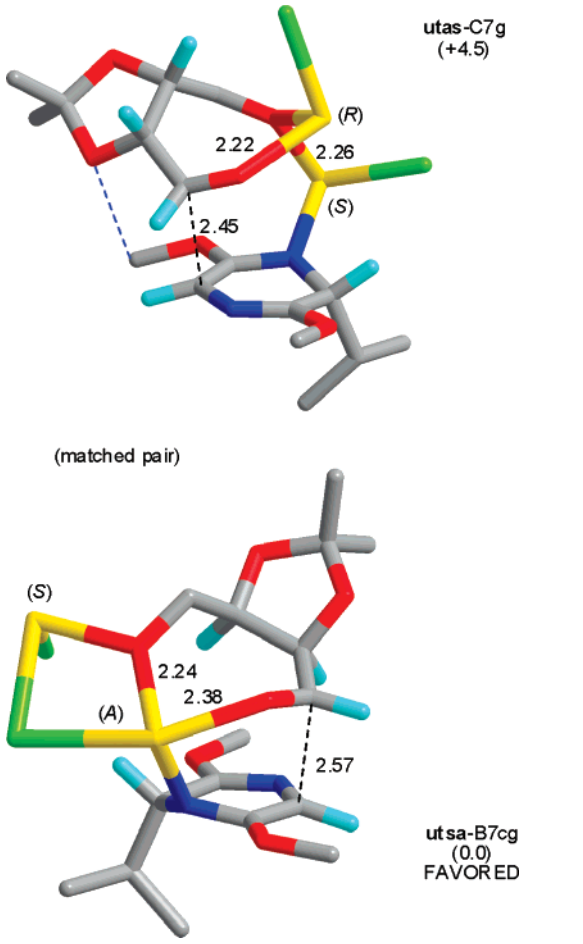

FIGURE 4. Chem3D representations of the most favored unsolvated TSs located (B3LYP/cc-pVDZ-PP level) for the aldol addition of unsolvated tin(II) azaenolate (**uA**) to D-erythrose acetonide (**De**). Relative energies in the gas phase (B3LYP/cc-pVTZ-PP level) are shown in parenthesis in kcal/mol. Distances are in angstroms. The hydrogen atoms are omitted for clarity except at chiral and reaction centers. Legend: carbon = gray, nitrogen = blue, oxygen = red, hydrogen = turquoise, tin = yellow, chlorine = green.

utsa-B7cg the pericyclic ring adopts a boat-like conformation, and the seven-membered chelate ring enables a Felkin−Anh conformation for the erythrose moiety. The additional four-membered ring originates from the simultaneous interaction of one chlorine and the *γ*-oxygen atom with both tin(II) cations. Most stable TSs located in the competing **tas**, **caa**, and **css** pathways were computed to be 4.5, 16.7, and 18.4 kcal/mol higher in energy than **utsa**-B7cg, respectively (see **utas**-C7g in Figure 4 and **ucaa**-C7c and **ucss**-C5c in Figure S6 and Table S6 of the Supporting Information), conveniently reproducing the high *trans*,*syn*,*anti*-diastereoselectivity observed in the addition of azaenolate $SnCl^{+}$**12**$^{-}$ to erythrose acetonide (*R*,*R*)-**19c** (see Table 3).

Reaction of **uA** with L-erythrose acetonide (*S*,*S*)-**19c** to give the mismatched complex **uALe** was also favored in the gas phase (see Table S7 in the Supporting Information). Full optimization of the selected geometries for **uALe** enabled the location of sets of TSs in the **cas**, **csa**, **taa**, and **tss** diastereomeric pathways for the mismatched aldol addition. The TS of lowest energy was found in the *trans*,*anti*,*anti* diastereomeric pathway, 19.3 kcal/mol above the intermediate complex. This TS, designated as **utaa**-C7c (see Figure 5) was characterized by the

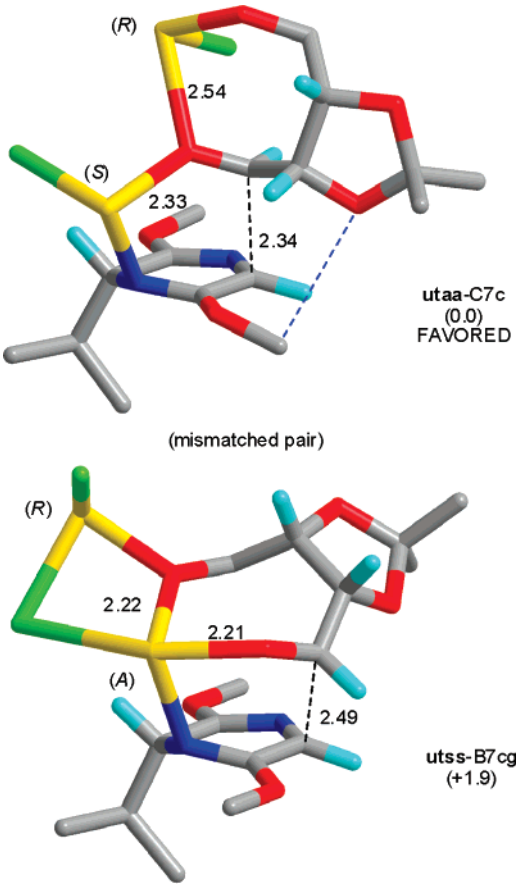

FIGURE 5. Chem3D representations of the most favored unsolvated TSs located (B3LYP/cc-pVDZ-PP level) for the aldol addition of unsolvated tin(II) azaenolate (**uA**) to L-erythrose acetonide (**Le**). Relative energies in the gas phase (B3LYP/cc-pVTZ-PP level) are shown in parenthesis in kcal/mol. Distances are in angstroms. The hydrogen atoms are omitted for clarity except at chiral and reaction centers. Legend: carbon = gray, nitrogen = blue, oxygen = red, hydrogen = turquoise, tin = yellow, chlorine = green.

presence of two pseudotetrahedral, tricoordinated tin(II) cations, a chair-like conformation for the pericyclic ring, and a Cornforth-like conformation for the erythrose moiety, which was also involved in a seven-membered chelate ring. Thus, in TS **utaa**-C7c the carbonyl oxygen acts as a bidentated ligand, which binds to the tin(II) cation of the azaenolate and also to the tin(II) cation of the erythrose moiety. The distance between a methoxy hydrogen of the bislactim and the oxygen at α-position of the erythrose moiety of **utaa**-C7c was 2.27 Å, which indicated a hydrogen bond. Most stable TS in the *trans*,*syn*,*syn* pathway was computed to be 1.9 kcal/mol higher in energy than **utaa**-C7c and showed a 4,6,7 ring system, with a boat-like conformation for the pericyclic ring and a Cornforth-like conformation for the erythrose moiety (see **utss**-B7cg in Figure 5). TSs in the *cis* pathways were computed to be more than 10 kcal/mol higher in energy (see **ucas**-B5c and **ucsa**-C7c in Figure S7 and Table S7 of the Supporting Information). Although the energy difference between **utaa**-C7c and the competitive TSs suggests a somewhat higher selectivity than the one observed experimentally for this specific reaction, it is qualitatively in agreement with the direction of the diastereofacial bias.

In summary, according to DFT calculations, the addition of tin(II) azaenolates to the erythrose acetonides proceeds by a three-step mechanism. The initial deprotonation of the erythrose

SCHEME 11

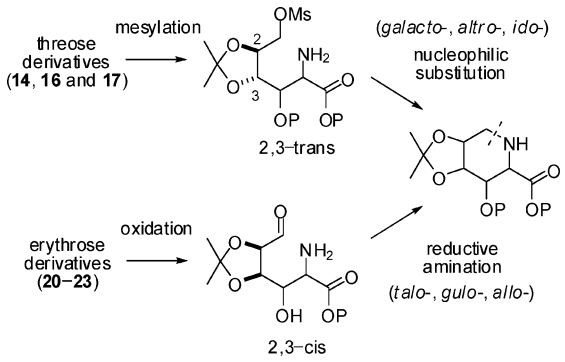

acetonide by the tin(II) azaenolate leading to a tin(II) alkoxy-derivative is followed by the addition to a second tin(II) azaenolate to form an intermediate complex. Final reorganization to the aldolates takes place through competing pericyclic TSs in which the erythrose moiety is preferentially involved in seven-membered chelate rings. The calculated TSs account for the experimentally observed stereoselectivities: *trans*,*syn*,*anti*-TS is favored for the matched pair and *trans*,*anti*,*anti*-TSs is favored for the mismatched one, and the energy gap between the competitive TSs is greater for the matched pair than for the mismatched one. Finally, the enhanced selectivity observed in the aldol addition of the mismatched tin(II) azaenolate to the "unprotected" erythrose acetonide **19c** relative to that obtained with the γ-benzylated erythrose acetonide **19a** (9:1 versus <2:1 *trans*,*anti*,*anti*/*trans*,*syn*,*syn* ratio) could be explained in terms of the conformational restriction of the erythrose moiety in the seven-membered chelate ring, which leads to tighter TSs and superior π-facial selectivity. In this manner, chelation appears to play a key role in both activating the "unprotected" erythrose moiety toward the aldol addition and directing facial selectivity.

3. Transformation of Aldol Adducts into 1-Deoxynojirimycins. Conversion of the aldol adducts into the targeted imino sugars required, in addition to the removal of the chiral auxiliary and reduction of the carboxylic acid group, the selective activation of the primary hydroxyl group that would enable the cyclization by intramolecular *N*-alkylation. Two different methodologies to carry out the cyclization of the threose and the erythrose derivatives were sought (see Scheme 11). Mesylation of the primary hydroxyl group and subsequent nucleophilic displacement by the amino group was appropriate for the cyclization of the threose derivatives, and the selective oxidation of the primary hydroxyl group followed by intramolecular reductive amination was successfully performed with the erythrose derivatives (see Schemes 12 and 14).

For the synthesis of the threose-derived imino sugars, additional amounts of the starting compounds **14b**, **16b**, and **17b** were obtained in excellent yields by catalytic hydrogenation (Pd/C, P atm, rt) of the benzylated adducts **14a**, **16a**, and **17a** followed by monosilylation (TBDPSCl, DMAP, Et_3N, CH_2Cl_2, rt, 24 h) of the corresponding diols **14c**, **16c**, and **17c** (see Schemes 2 and 3). Orthogonal protection of the secondary hydroxyl group of the silylated adducts **14b**, **16b**, and **17b** was deemed, in order to avoid competitive ring-closure processes to furan derivatives. In this way, treatment of compounds **14b**, **16b**, and **17b** with sodium hydride and benzyl bromide in the presence of a catalytic amount of tetrabutylammonium iodide led to the corresponding benzyl ethers **24b**, **25b**, and **26b**, respectively, in good yields (see Scheme 12). After deprotection of the silyl ether under standard conditions, the mesylation of

SCHEME 12 [a]

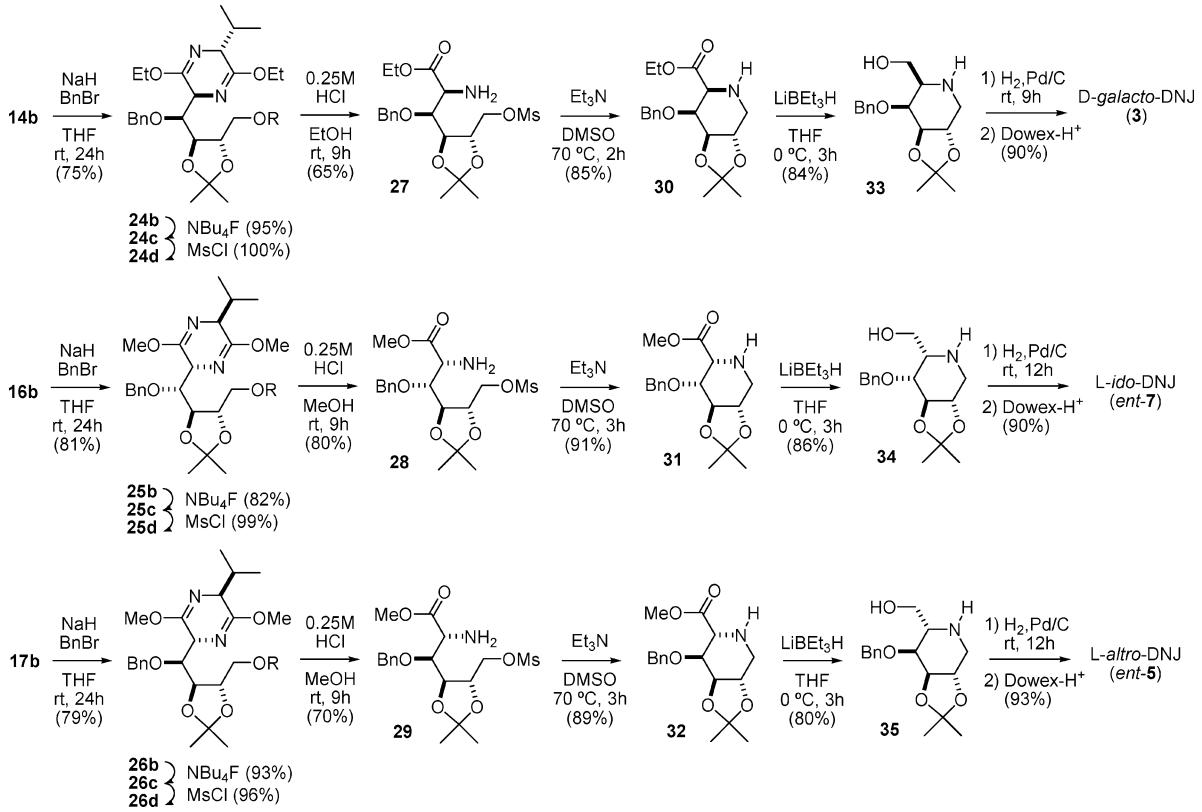

[a] Legend: **b**, R = $SiPh_2{}^tBu$; **c**, R = H; **d**, R = Ms.

the alcohols **24c**, **25c**, or **26c** was accomplished in almost quantitative yields. Selective hydrolysis of the pyrazino moiety of the mesylates **24d**, **25d**, or **26d**, in the presence of the isopropylidene ketal, took place without cyclization and furnished the amino mesylates **27**, **28**, and **29** in good yields. Although the amino mesylates underwent a slow conversion to the corresponding pipecolates **30**, **31**, and **32** on standing, cyclizations were completed by heating the amino mesylates in dimethylsulfoxide, using triethylamine as an auxiliary base. Reduction of the pipecolates **30**, **31**, and **32** with lithium triethylborohydride proceeded cleanly, as previously described for other piperidine derivatives with acidic functionality,[56] and the hydroxypiperidines **33**, **34**, and **35** were isolated in good yields. Finally, deprotection of intermediates **33**, **34**, and **35** by catalytic hydrogenation in acidic media (THF/HCl 0.25N 1:1) and purification of the crude reactions by ion-exchange chromatography (Dowex, H^+ form) and reversed-phase flash chromatography led to the isolation of the corresponding imino sugars, 1-deoxy-D-galactonojirimycin, 1-deoxy-L-idonojirimycin, and 1-deoxy-L-altronojirimycin (**3**, *ent*-**7** and *ent*-**5**, respectively; see Scheme 12 and Charts 1 and 2) in high yields.

Pipecolic acid **36**, an analogue of galacturonic acid that has shown a potent inhibition of several α-galactosidases and galacturonases,[57] was also readily available from the pipecolate **30** (see Scheme 13). Thus, under the conditions employed for deprotection of the piperidines, **30** gave rise to the pipecolic acid **36**, which could be isolated in excellent yield after ion-exchange and reversed-phase flash chromatography.

SCHEME 13

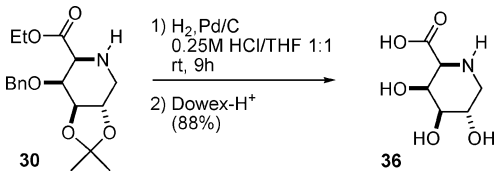

Conversion of the erythrose-derived adducts **20a,c**, **21a,c**, **22a,c**, and **23a,c** into 1-deoxy-D-talonojirimycin, 1-deoxy-D-allonojirimycin, 1-deoxy-D-gulonojirimycin, and 1-deoxy-L-talonojirimycin, respectively, is straightforward, as depicted in Scheme 14. In order to avoid unnecessary protection−deprotection steps, a chemoselective oxidation of the primary alcohol in the presence of a secondary one was required. Thus, debenzylation of adducts **20a**, **21a**, **22a**, and **23a** by catalytic hydrogenation gave additional amounts of the corresponding diols **20c**, **21c**, **22c**, and **23c** in quantitative yields (see Schemes 4 and 5), which were subsequently oxidized to the γ-lactols **37**, **38**, **39**, and **40**, respectively, by using a slight modification of Corey's conditions.[58,59] In this way, when a solution of compound **20c**, **21c**, **22c**, or **23c** in THF was treated with a

(56) See for example: Shilvock, J. P.; Wheatley, J. R.; Davis, B.; Nash, R. J.; Griffiths, R. C.; Jones, M. G.; Müller, M.; Crook, S.; Watkin, D. J.; Smith, C.; Besra, G. S.; Brennan, P. J.; Fleet, G. W. J. *Tetrahedron Lett.* **1996**, *37*, 8569−8572.

(57) Tong, M. K.; Blumenthal, E. M.; Ganem, B. *Tetrahedron Lett.* **1990**, *31*, 1683−1684. Other trihydroxypipecolic acids have shown important biological activities: (a) Le Merrer, Y.; Poitout, L.; Depezay, J.-C.; Dosbaa, I.; Geoffroy, S.; Foglietti, M.-J. *Bioorg. Med. Chem.* **1997**, *5*, 519−533. (b) Tsuruoka, T.; Fukuyasu, H.; Ishii, M.; Usui, T.; Shibahara, S.; Inouye, S. *J. Antibiot.* **1996**, *49*, 155−61. (c) Fleet, G. W. J.; Karpas, A.; Dwek, R. A.; Fellows, L. E.; Tyms, A. S.; Petursson, S.; Namgoong, S. K.; Ramsden, N. G.; Smith, P. W.; Son, J. C.; Wilson, F.; Witty, D. R.; Jacob, G. S.; Rademacher, T. W. *FEBS Lett.* **1988**, *237*, 128−32.

(58) Corey, E. J.; Palani, A. *Tetrahedron Lett.* **1995**, *36*, 3485−3488.

SCHEME 14 [a]

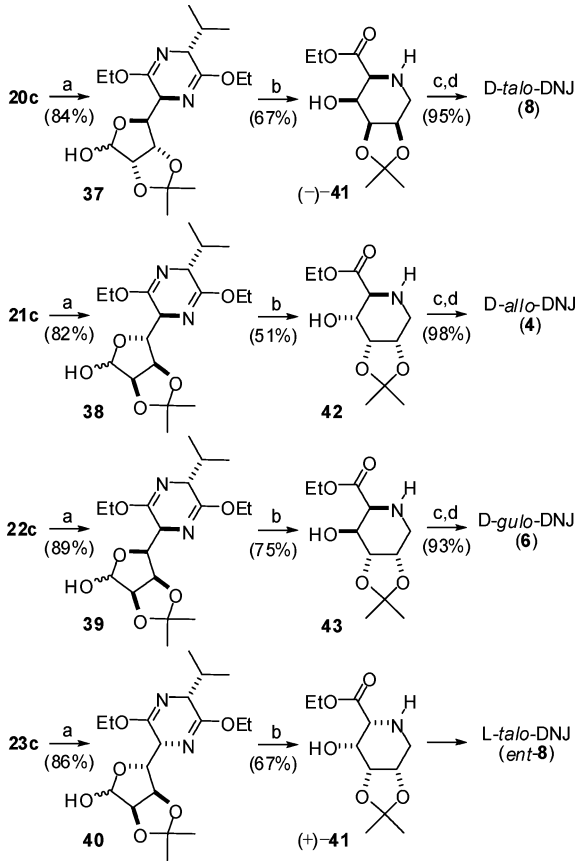

[a] Reagents and conditions: (a) IBX, DMSO/THF (1:1), 8 °C, 24 h. (b) 0.25 M HCl/EtOH (1:2), H_2, Pd/C, rt, 4 h. (c) $LiBEt_3H$, THF, rt, 3 h. (d) Dowex-H^+.

solution of *o*-iodoxybenzoic acid (IBX)[60] in DMSO, a 62−68% conversion to the desired lactols **37**, **38**, **39**, or **40** was achieved. As the overoxidation to the corresponding lactones was completely suppressed, the yield of lactols **37**−**40** could be increased to 82−89% by resubjecting recovered starting materials to these oxidation conditions. Selective hydrolysis of the bislactim ether in the presence of the isopropylidene ketal and subsequent intramolecular reductive amination were achieved in a one-pot procedure. Stirring the lactols **37**, **38**, **39**, or **40** in a 1:2 mixture of 0.25 M HCl and EtOH under a hydrogen atmosphere and palladium catalyst afforded the piperidine esters (−)-**41**, **42**, **43**, or (+)-**41** in good yields. Reduction of (−)-**41**, **42**, or **43** with $LiBEt_3H$ also proceeded cleanly. Filtering of the reduction crudes through Dowex (H^+ form) and purification by reversed-phase flash chromatography afforded 1-deoxy-D-talononojirimycin, 1-deoxy-D-allonojirimycin, or 1-deoxy-D-gulonojirimycin in excellent yields (**8**, **4**, and **6**, respectively; see Scheme 14 and Chart 2). Specific rotations and spectral data obtained for imino sugars **3**−**8** were consistent with the literature values (see Supporting Information).

In conclusion, we have demonstrated the utility of aldol additions of metalated bislactim ethers to threose or erythrose acetonides in the synthesis of 1,5-iminohexitols related to 1-deoxynojirimycin. The easy availability of the reagents, the stereoselectivity in the aldol processes of matched and mismatched pairs, and the good yield of the steps would give easy access for the synthesis of new polyhydroxylated alkaloids that may be useful for glycosidase inhibition and development of beneficial drugs. Additional studies to adapt this aldol-based strategy to the synthesis of 2,5-iminohexitols are currently under investigation and will be reported in due course.

Experimental Section

General Procedure 1 for Aldol Addition. Method A. A solution of *n*-BuLi (1.2 equiv, 2.5 M in hexane) was added to a stirred solution of Schöllkopf's bislactim ether (1.2 equiv) in THF (10 mL/mmol) at −78 °C, and the mixture was stirred for 1 h. Then, a 0.5 M solution of the additive ($ZnCl_2$, $SnCl_2$, $Sn(OTf)_2$, Et_2AlCl, $MgBr_2$·OEt, $Ti(O^iPr)_3Cl$, or $Ti(NEt_2)_3Cl$) in THF (1.2−2.4 equiv) was added dropwise. The mixture was stirred for 1 h, and a solution of aldehyde (1.0 equiv) in THF (2.5−4.0 mL/mmol) was added dropwise. After being stirred at −78 °C for 2 h, the reaction was quenched with aqueous saturated NH_4Cl or $NaHCO_3$ solution. The crude reaction mixture was warmed to room temperature, and the solvent was removed in vacuo. The resulting material was diluted with water and extracted with ether. The combined organic layers were dried (Na_2SO_4) and evaporated, and the residue was purified by flash chromatography (silica gel, EtOAc/hexanes from 1:9 to 3:1 ratio) to yield the corresponding addition products. **Method B.** A solution of *n*-BuLi (3.0 equiv, 2.5 M in hexane) was added to a stirred solution of Schöllkopf's bislactim ether (3.0 equiv) in THF (10 mL/mmol) at −78 °C, and the mixture was stirred for 1 h. Then, a 0.5 M solution of the additive ($ZnCl_2$, $SnCl_2$, $MgBr_2$·OEt, $Ti(O^iPr)_3Cl$, $Ti(NEt_2)_3Cl$, or TMSCl and $SnCl_4$) in THF (3.0−6.0 equiv) was added dropwise. The mixture was stirred for 1 h, and a solution of lactol (1.0 equiv) in THF (2.5−4.0 mL/mmol) was added dropwise. The reaction mixture was gradually warmed to 0 °C for 5−12 h, and the reaction was quenched with aqueous NH_4Cl or saturated $NaHCO_3$ solution and worked up as described in method A.

(3*S*,6*R*,1′*S*,2′*S*,3′*S*)-3-[4-Benzyloxy-1-hydroxy-2,3-isopropylidenedioxybutyl]-2,5-diethoxy-3,6-dihydro-6-isopropylpyrazine (14a). Following method A of the general procedure 1, reaction of (*R*)-**12** (314 mg, 1.48 mmol) with **13a** (308 mg, 1.23 mmol) using $SnCl_2$ as additive (280 mg, 1.48 mmol) gave, after flash chromatography (silica gel, EtOAc/hexanes from 1:9 to 1:4 ratio), 460 mg of adduct **14a** (81%). Colorless oil; R_f = 0.67 (EtOAc/hexanes 1:2); $[\alpha]^{29}_D$ −5.2 (*c* 1.1, CH_2Cl_2); IR (film) ν 3450, 2973, 1695, 1480, 1369, 1233 cm^{-1}; ^1H NMR ($CDCl_3$) δ 0.76 (d, J = 6.8 Hz, 3H), 1.04 (d, J = 6.8 Hz, 3H), 1.23−1.34 (m, 6H), 1.45 (s, 6H), 2.21 (dsp, J = 6.8, 3.4 Hz, 1H), 3.67 (d, J = 5.4 Hz, 2H), 3.97 (t, J = 3.4 Hz, 1H), 4.03−4.31 (m, 8H), 4.61 (s, 2H), 7.27−7.35 (m, 5H); ^{13}C NMR ($CDCl_3$) δ 14.3 (CH_3), 17.0 (CH_3), 19.1 (CH_3), 27.1 (CH_3), 27.2 (CH_3), 32.2 (CH), 56.5 (CH), 60.8 (CH_2), 61.1 (CH), 71.2 (CH_2), 72.9 (CH), 73.4 (CH_2), 76.4 (CH), 78.9 (CH), 109.5 (C), 127.6 (CH), 128.3 (CH), 137.8 (C), 161.2 (C), 166.0 (C); FABMS (thioglycerol) *m*/*z* 463 (MH^+, 85). Anal. Calcd for $C_{25}H_{38}N_2O_6$: C, 64.91; H, 8.28; N, 6.06. Found: C, 64.75; H, 8.38; N, 6.00.

(3*S*,6*R*,1′*S*,2′*S*,3′*S*)-3-[4-*tert*-Butyldiphenylsilyloxy-1-hydroxy-2,3-isopropylidenedioxybutyl]-2,5-diethoxy-3,6-dihydro-6-isopropylpyrazine (14b). Following method A of the general procedure 1, reaction of (*R*)-**12** (0.96 g, 4.52 mmol) with **13b** (1.5 g, 3.77 mmol) using $SnCl_2$ as additive (0.86 g, 4.52 mmol) gave, after flash chromatography (silica gel, EtOAc/hexanes from 1:9 to 1:3

(59) Attempts to obtain the γ-lactols by treatment of the diols in the conditions reported by Kim (NCS, iPr_2S, Et_3N, CH_2Cl_2, 0 °C) or Skarzewski (TEMPO, NaOCl, CH_2Cl_2, from 0 °C to rt) were unsuccessful. (a) Kim, K. S.; Cho, I. H.; Yoo, B. K.; Song, Y. H.; Hahn, C. S. *J. Chem. Soc., Chem. Commun.* **1984**, 762−763. (b) Siedlecka, R.; Skarzewski, J.; Mlochowski, J. *Tetrahedron Lett.* **1990**, *31*, 2177−2180.

(60) IBX was prepared as described in: Frigerio, M.; Santagostino, M.; Sputore, S.; Palmisano, G. *J. Org. Chem.* **1995**, *60*, 7272−7276. CAUTION: IBX has been reported to detonate upon heavy impact and heating over 200 °C: (a) Plumb, J. B.; Harper D. J. *Chem. Eng. News* **1990**, July 16, 3. See also: (b) Dess, B. D.; Martin, J. C. *J. Am. Chem. Soc.* **1991**, *113*, 7277−7287.

ratio), 1.74 g of adduct **14b** (75%). Compound **14b** was also prepared according to the general procedure 3 (see Supporting Information); silylation of **14c** (350 mg, 0.94 mmol) gave 562 mg of **14b** (98%). Colorless oil; $R_f = 0.35$ (EtOAc/hexanes 1:9); $[\alpha]^{20}_D$ −8.5 (*c* 2.0, CH_2Cl_2); IR (film) ν 3450, 2900, 1700, 1480, 1380, 1250, 1100 cm^{-1}; ^1H NMR (300 MHz, $CDCl_3$) δ 0.77 (d, $J = 6.8$ Hz, 3H), 1.04 (d, $J = 6.8$ Hz, 3H), 1.05 (s, 9H), 1.23 (t, $J = 7.3$ Hz, 3H), 1.31 (t, $J = 7.3$ Hz, 3H), 1.45 (s, 6H), 2.02 (d, $J = 9.3$ Hz, 1H), 2.25 (dsp, $J = 6.8$, 3.9 Hz, 1H), 3.84 (d, $J = 4.4$ Hz, 2H), 3.98 (t, $J = 3.9$ Hz, 1H); 4.01−4.28 (m, 7H); 4.40 (dd, $J = 8.8$, 6.3 Hz, 1H), 7.33−7.44 (m, 6H), 7.66−7.73 (m, 4H); ^{13}C NMR ($CDCl_3$) δ 14.3 (CH_3), 17.1 (CH_3), 19.1 (CH_3), 19.2 (CH_3), 19.2 (C), 26.7 (CH_3), 27.4 (CH_3), 32.3 (CH), 56.5 (CH), 60.8 (CH_2), 60.9 (CH_2), 61.1 (CH), 64.5 (CH_2), 73.1 (CH), 76.4 (CH), 80.4 (CH), 109.4 (C), 127.7 (CH), 129.7 (CH), 133.1 (C), 135.6 (CH), 161.3 (C), 166.2 (C); FABMS (thioglycerol) *m*/*z* 611 (MH^+, 40). Anal. Calcd for $C_{34}H_{50}N_2O_6Si$: C, 66.85; H, 8.25; N, 4.59. Found: C, 66.62; H, 8.56; N, 4.36.

(3*S*,6*R*,1′*S*,2′*S*,3′*S*)-3-[1,4-Dihydroxy-2,3-isopropylidenedioxybutyl]-2,5-diethoxy-3,6-dihydro-6-isopropylpyrazine (14c). Following method B of the general procedure 1, reaction of (*R*)-**12** (388 mg, 1.83 mmol) with **13c** (98 mg, 0.61 mmol) using $SnCl_2$ as additive (347 mg, 1.83 mmol) gave, after flash chromatography (silica gel, EtOAc/hexanes from 1:9 to 2:1 ratio), 150 mg of adduct **14c** (66%). Compound **14c** was also prepared according to the general procedure 2 (see Supporting Information); hydrogenation of **14a** (350 mg, 0.76 mmol) gave 282 mg of **14c** (100%). Colorless solid; mp (EtOAc/hexanes) 67−69 °C; $R_f = 0.28$ (EtOAc/hexanes 1:1); $[\alpha]^{27}_D$ −15.4 (*c* 1.0, CH_2Cl_2); IR (KBr) ν 3384, 2972, 1698, 1233, 1035 cm^{-1}; ^1H NMR ($CDCl_3$) δ 0.76 (d, $J = 6.8$ Hz, 3H), 1.04 (d, $J = 6.8$ Hz, 3H), 1.29 (t, $J = 6.8$ Hz, 3H), 1.30 (t, $J = 6.8$ Hz, 3H), 1.45 (s, 6H), 2.1 (brd, 1H), 2.24 (dsp, $J = 6.8$, 3.6 Hz, 1H), 2.77 (brs, 1H), 3.75−3.85 (m, 2H), 3.98 (t, $J = 3.6$ Hz, 1H); 4.06−4.28 (m, 8H); ^{13}C NMR ($CDCl_3$) δ 14.2 (CH_3), 14.2 (CH_3), 17.0 (CH_3), 19.1 (CH_3), 27.0 (CH_3), 27.1 (CH_3), 32.3 (CH), 56.4 (CH), 61.2 (CH_2), 61.2 (CH), 63.5 (CH_2), 72.4 (CH), 77.8 (CH), 79.8 (CH), 109.0 (C), 160.9 (C), 166.7 (C); FABMS (thioglycerol) *m*/*z* 373 (MH^+, 100). Anal. Calcd for $C_{18}H_{32}N_2O_6$: C, 58.05; H, 8.66; N, 7.52. Found: C, 58.31; H, 8.60; N, 7.44.

(3*S*,6*R*,1′*S*,2′*S*,3′*R*)-3-[4-Benzyloxy-1-hydroxy-2,3-isopropylidenedioxybutyl]-2,5-diethoxy-3,6-dihydro-6-isopropylpyrazine (20a). Following method A of the general procedure 1, reaction of (*R*)-**12** (300 mg, 1.41 mmol) with (*R*,*R*)-**19a** (293 mg, 1.17 mmol) using $SnCl_2$ as additive (267 mg, 1.41 mmol) gave, after flash chromatography (silica gel, EtOAc/hexanes from 1:9 to 1:4 ratio), 395 mg of adduct **20a** (73%). Colorless oil; $R_f = 0.67$ (EtOAc/hexanes 1:2); $[\alpha]^{29}_D$ +11.9 (*c* 1.0, CH_2Cl_2); IR (film) ν 2980, 2933, 1697, 1235, 1074 cm^{-1}; ^1H NMR (300 MHz, $CDCl_3$) δ 0.74 (d, $J = 6.8$ Hz, 3H), 1.04 (d, $J = 6.8$ Hz, 3H), 1.27 (t, $J = 6.8$ Hz, 3H), 1.30 (t, $J = 6.8$ Hz, 3H), 1.40 (s, 3H), 1.46 (s, 3H), 2.27 (dsp, $J = 6.8$, 3.5 Hz, 1H), 2.75 (d, $J = 7.1$ Hz, 1H), 3.62 (dd, $J = 9.9$, 5.3 Hz, 1H), 3.82 (dd, $J = 9.9$, 6.9 Hz, 1H), 3.97 (t, $J = 3.5$ Hz, 1H), 4.12−4.28 (m, 6H), 4.44−4.48 (m, 2H), 4.56/4.63 (AB system, $J = 11.8$ Hz, 2H), 7.26−7.35 (m, 5H); ^{13}C NMR (75 MHz, $CDCl_3$) δ 14.3 (CH_3), 14.4 (CH_3), 16.9 (CH_3), 19.1 (CH_3), 25.6 (CH_3), 28.1 (CH_3), 32.0 (CH), 56.4 (CH), 60.7 (CH_2), 60.8 (CH_2), 60.9 (CH), 68.7 (CH_2), 69.1 (CH), 73.8 (CH_2), 75.8 (CH), 76.0 (CH), 108.6 (C), 127.9 (CH), 128.5 (CH), 137.3 (C), 161.2 (C), 165.3 (C); FABMS (thioglycerol) *m*/*z* 463 (MH^+, 100), 165 (51). Anal. Calcd for $C_{25}H_{38}N_2O_6$: C, 64.91; H, 8.28; N, 6.06. Found: C, 65.10; H, 8.21; N, 6.23.

(3*S*,6*R*,1′*S*,2′*S*,3′*R*)-3-[1,4-dihydroxy-2,3-isopropylidenedioxybutyl]-2,5-diethoxy-3,6-dihydro-6-isopropylpyrazine (20c). Following method B of the general procedure 1, reaction of (*R*)-**12** (3.58 g, 16.87 mmol) with (*R*,*R*)-**19c** (900 mg, 5.62 mmol) using $SnCl_2$ as additive (3.20 g, 16.87 mmol) gave, after flash chromatography (silica gel, EtOAc/hexanes from 1:4 to 2:3 ratio), 1.94 g of adduct **20c** (93%). Compound **20c** was also prepared according to the general procedure 2 (see Supporting Information); hydrogenation of **20a** (350 mg, 0.76 mmol) gave 281 mg of **20c** (100%). Colorless oil; $R_f = 0.31$ (EtOAc/hexanes 1:3); $[\alpha]^{23}_D$ −69.0 (*c* 0.5, CH_2Cl_2); IR (film) ν 3395, 2978, 1693, 1459, 1381, 1237, 1144, 1036 cm^{-1}; ^1H NMR ($CDCl_3$) δ 0.76 (d, $J = 6.8$ Hz, 3H), 1.02 (d, $J = 6.8$ Hz, 3H), 1.28 (t, $J = 6.8$ Hz, 3H), 1.29 (t, $J = 6.8$ Hz, 3H), 1.39 (s, 3H), 1.46 (s, 3H), 2.22 (dsp, $J = 6.8$, 3.9 Hz, 1H), 2.49 (brd, $J = 8.3$ Hz, 1H), 3.07 (brt, $J = 5.9$ Hz, 1H), 3.75−4.00 (m, 2H), 3.97 (t, $J = 3.9$ Hz, 1H), 4.03−4.42 (m, 8H); ^{13}C NMR ($CDCl_3$) δ 14.2 (CH_3), 17.1 (CH_3), 19.0 (CH_3), 25.5 (CH_3), 27.9 (CH_3), 32.3 (CH), 55.9 (CH), 60.6 (CH_2), 60.9 (CH_2), 61.1 (CH), 69.1 (CH), 75.8 (CH), 77.4 (CH), 108.4 (C), 161.4 (C), 166.3 (C); FABMS (thioglycerol) *m*/*z* 373 (MH^+, 100). Anal. Calcd for $C_{18}H_{32}N_2O_6$: C, 58.05; H, 8.66; N, 7.52. Found: C, 58.31; H, 8.39; N, 7.28.

Acknowledgment. We gratefully acknowledge Ministerio de Ciencia y Tecnología (BQU2003-00692) and Xunta de Galicia (PGIDIT05BTF10301PR) for financial support, Novartis Pharma for the generous gift of bislactim ethers derived from *cyclo*-[Val-Gly], and Noa Castro and Isaac Vázquez for technical assistance. The authors are indebted to Centro de Supercomputación de Galicia for providing the computer facilities. O.B. thanks Xunta de Galicia for an "Isidro Parga Pondal" position at Universidade da Coruña.

Supporting Information Available: Experimental procedures and full characterization of new compounds and computational methods, Cartesian coordinates, and absolute energies for all models reported. This material is available free of charge via the Internet at http://pubs.acs.org.

JO702601Z